ELECTROPHYSIOLOGY AND PHARMACOLOGY OF PERSISTENT SODIUM CURRENTS PRESENT IN THE MAMMALIAN BRAIN

Adriana M. Galue

Department of Neurology and Neurosurgery

McGill University, Montreal

A Thesis submitted to the Faculty of Graduate Studies and Research in partial fulfilment of the requirements of the degree Master of Science

May 1998

ABSTRACT

Persistent sodium conductances are important both in normal and pathological brain states. In the first part of the present study we characterized a Type of persistent sodium conductance (I_{Nap}) present in stellate cell neurons of the layer II medial entorhinal cortex area of the rat brain. To accomplish this task, we used the whole-cell configuration of the patch clamp technique to record sodium currents in dissociated entorhinal neurons. It was found that I_{Nap} represents 5 to 10% of the amplitude of the fast inactiuvating sodium conductance (I_{NaF}). In addition, I_{Nap} activates at potentials 10mV more negative than I_{NaF}, and this persistent conductance is present at potentials more positive than those expected for a window current. These results show that I_{Nap} in entorhinal neurons is due to a distinct subset of non-inactivating sodium channels, rather than a window current.

In the second part of the study, we carried out a pharmacological characterization of the Type III sodium channel, which is a molecular model to study persistent conductances. We tested the actions of phenytoin, carbamazepine, tetracaine and topiramate on these channels when expressed in the *Xenopus* oocyte system using the two-electrode double-voltage recording technique. It was found that all the drugs except topiramate, block the Type III currents in a voltage dependent manner. The sensitivity of Type III currents to drugs was not affected by coexpression of auxiliary sodium channel β subunits, and it was similar to the sensitivity of fast-inactivating Type IIA sodium channels.

RESUME

Les conductances persistantes de sodium jouent un rôle très important dans des conditions normales et pathologiques du cerveau. Dans la première partie de cette étude, nous avons caracterisé un Type de conductance sodique persistante (I_{Nap}) dans des neurones étoilées (niveau II) du cortex entorhinal median du cerveau de rat. Pour accomplir ce travail, nous avons utilisé des neurones entorhinauses dissociées et employé la technique dite du "patch-clamp" sur cellule entière. Les resultats montrent que l'amplitude de l' I_{Nap} represente entre 5 et 10% de l'amplitude de la courant transitoire de sodium dans les mêmes neurones (I_{Naf}). De plus, I_{Nap} s'active à un potentiel qui est 10mV inferieur au potentiel d'activation de l' I_{Naf} . Aussi, cette conductance persistente est presente à des potentiels superieurs à ceux habituellement observés pour des courants "window". Ces resultats démontrent que l' I_{Nap} observée dans les neurones entorhinaux peut être dûe à l'activation d'un ensemble distinct de canaux sodium.

Dans la deuxième partie de cet étude, nous avons caracterisé pharmacologiquement le canal sodique de Type III. Ce canal est un modèle moléculaire d' étude des conductances persistantes de sodium. Nous avons testé les effets d'antiépileptiques tels que la phénytoin, la carbamazepine et le topiramate, ainsi que les effets d'un anesthetique, la tetracaine. Cette étude a été menée sur oocytes de *Xenopus* exprimant ce canal, et la technique d'enregistrement a deux electrodes a été utilisé. Il a ainsi été demontré que tous les agents pharmacologiques à l'exception du topiramate, inhibent ce canal de manière voltage dependante. Cette inhibition est depandent du potentiel de la membrane. La sensibilité du canal de Type III aux drogues utilisés, n'est pas affecté par la coexpression des sous-unités β. Cette sensitivité à ete similaire à celle des canaux sodium Type IIA.

EXPLANATORY NOTE

The following is a required excerpt from the McGill University Faculty of Graduate Studies and Research: *Guidelines Concerning Thesis Preparation:*

Candidates have the option of including, as part of the thesis, the text of one or more papers submitted or to be submitted for publication, or the clearly-duplicated text of one or more published papers. These texts must be bound as an integral part of the thesis.

If this option is chosen, connecting texts that provide logical bridges between the different papers are mandatory. The theisi must be written in such a way that it is more than a mere collection of manuscripts; in other words, results of a series of papers must be integrated.

The thesis must still conform to all other requirements of the "Guidelines for Thesis Preparation". The thesis must include: A Table of Contents, an abstract in English and French, an introduction which clearly states the rationale and objectives of the work, a review of the literature, a final conclusion and summary, and a thorough bibliography or reference list.

Additional material must be provided where appropriate (e.g. in appendices) and in sufficient detail to allow a clear and precise judgement to be made of the importance and originality of the research reported in the thesis.

In the case of manuscripts co-authored by the candidate and others, the candidate is required to make explicit statement in the thesis as to who contributed to such work and to what extent.
Supervisors must attest to the accuracy of such statement at the doctoral oral defense. Since the task of the examiners is made more difficult in these cases, it is in the candidate's interest to make perfectly clear the responsibilities of all the authors of the co-authored papers.

This work is part of the ongoing research on the electrical properties of neurons present in the entorhinal cortex underway in the laboratory of Dr. Angel Alonso. Also as part of the ongoing research on the pharmacological and molecular properties of Type III channels underway in the laboratory of Dr. David Ragsdale. The first part of the work was written entirely by myself, including methods and results. The second part was written with the help of Dr David Ragsdale. The whole body of this work was revised by Drs. Massimo Avoli, Peter McPherson and David Ragsdale.

ACKNOWLEDGEMENTS

I am grateful to God for having helped me through out my work.

I dedicate this thesis to my mother without whom I would have not achieved what I have.

I would like to thank my supervisor, Dr. David Ragsdale, to whom I am indebted for many reasons. I am grateful for his general encouragement and his patient and positive teaching style. It was an excellent learning experience to be under his supervision.
I would also like to thank Dr. Angel Alonso for having me be part of his laboratory and for the encouragement he gave me to pursue towards a goal.
I am especially grateful to Laurence Meadows, Dr. Ruby Klink and Isabelle for their support at all times, for their advice and help. I learned a lot from them.
To Nina, Armando, Steven, Fernando, Roger and Carolina for their true friendship and moral support. To Amy for helping me discover a new way to conceive life.
To Ivan, Mao and Mark for helping me dealing with technology.
I appreciated the guidance given by Dr. Peter McPherson and Dr. Massimo Avoli members of my graduate committee.
Finally I am grateful to life and to the rest of my family. To the composers of tropical rhythms. Music really complemented my daily struggle with electrodes and other electronic equipment.
This work was founded by the Medical Research Council of Canada, a grant given to Drs. Angel Alonso and David Ragsdale.

TABLE OF CONTENTS

PART TWO.

Pharmacology of Type III Na^+ Channels

SUMMARY AND CONCLUSIONS

1. The occurrence of persistent sodium currents is ubiquitous in the mammalian brain. In the present study, we characterized electrophysiologically a persistent sodium conductance present in medial entorhinal cortex layer II neurons of the rat brain.

2. The study was performed by using the whole cell configuration of the patch clamp technique on acutely dissociated neurons.

3. It was found that the persistent conductance activated at potentials 10 mV more negative than the fast inactivating sodium current. The amplitude of the persistent conductance ranged between 5 and 10% of the amplitude of the fast inactivating current. Furthermore, the sustained nature of these currents was detected even after 16 seconds after initiation of the pulse. This is in contrast to the fast inactivating sodium currents which inactivate within 4 ms.

4. The activation range of the persistent conductance was compared with that of the fast-inactivating current. It appears that persistent currents result from activation of a different sodium channel subtype.

5. In the second part of the study, we characterized pharmacologically the Type III sodium channel which produces persistent sodium currents.

6. We tested the actions of phenytoin, carbamazepine and topiramate which are widely known anticonvulsants. We also tested the actions of the anesthetic tetracaine.

7. It was found that Type III channels are blocked by these pharmacological agents in a voltage-dependent manner.

8. In contrast to our expectations, the newly developed anticonvulsant topiramate had no effect on the magnitude of the currents, suggesting that its mode of action is not via block of persistent sodium conductances.

9. When the Type III α subunit was coexpressed with its auxiliary subunits $\beta 1$ and $\beta 2$, the sensitivity of the channels for the drugs was not altered.

10. As means of comparison, similar type of experiments were performed using the fast-inactivating type of channel rII. Despite differences in the kinetic properties of inactivation between Type III and Type II channels, they both displayed similar sensitivities to local anesthetics and anticonvulsant drugs.

OVERVIEW

Sodium channels are voltage sensitive ion channels needed for the generation of action potentials in excitable cells (Catteral 1992). Sodium channels are also important for the variety of responses that a cell can generate due to its intrinsic electrophysiological properties (Llinas 1988). In the brain, sodium currents have diverse properties. For example, non-inactivating persistent sodium currents mediate subthreshold oscillations and amplification of synaptic potentials which alter cell firing frequency (Taylor 1993; Crill 1996). The present study has two parts. The first provides a basic characterization of a persistent sodium current present in entorhinal neurons. The second gives an initial pharmacological characterization of a model to study persistent sodium currents .

Background

Sodium Channel Function

In brain neurons, sodium channels lead to currents that are regulated by changes in membrane potential (Gonoi and Hille 1987; Patlak 1991). Resting neurons have a characteristic hyperpolarized membrane potential at which sodium channels are in a closed conformational state. Upon depolarization of the membrane, channels convert initially to an open state that allows influx of sodium ions, and then to a nonconductive inactivated state (Bezanilla and Armstrong 1977; Stuhmer, Conti et al. 1989) (FIG 1). The ability of these channels to cycle very rapidly between closed, open and inactivated states is critical for their ability to propagate the rapid trains of action potentials necessary for information processing in the brain.

Sodium Channel Structure

In the mammalian brain, sodium channels are formed by 3 subunits designated α, β1 and β2 (Catteral 1995). The α subunit is the main structural component of the channel and consists of four homologous structural domains (designated I, II, III, and IV). Analysis of the peptide sequence suggests that each domain consists of six putative transmembrane helices (S1-S6). The four domains associate in a square-like array to form the ion-conducting pore as shown in FIG 2.

PART ONE

A PERSISTENT NA^+ CURRENT PRESENT IN MEDIAL ENTORHINAL CORTEX LAYER II NEURONS.

Structure of the Entorhinal Cortex

The entorhinal cortex (EC) is a seven layer structure that connects the hippocampal formation with the rest of the cerebral cortex (Ramon y Cajal 1911; Lorente de No 1933). Layers II and III receive input from a variety of associational cortices. The output of these two layers constitutes the perforant path, which is the major cortical afferent projection to the hippocampal formation (Steward 1976; Steward and Scoville 1976; Ruth, Collier et al. 1982). In turn, the hippocampal formation projects back on the deep layers of the EC (V-VI) (Amaral and Insausti 1990; Jones 1993) as illustrated in FIG 3A.

The entorhinal cortex is an important structure from several points of view. First, it has been shown that its damage is responsible for many of the memory impairment

characteristics of Alzheimer's disease (Van Hoesen 1991). In fact, the EC is the earliest and most severely damaged of all cortical structures in this disease (Hyman, Van Hosen et al. 1990; Gomez-Isla, Price et al. 1996). Such degeneration is selective in terms of the layers affected. Superficial layers, particularly layers II and IV are strongly affected. Therefore, early memory changes characteristic of Alzheimer's disease, such as confusion and inability to recall new daily events, are probably related to the pathological changes that take place in the entorhinal cortex (Hyman, Van Hoesen et al. 1986a; Hyman, Van Hoesen et al. 1986b). Recent *in-vitro* studies suggest that the EC also can play an important role in temporal lobe epilepsy (Dasheiff and McNamara 1982; Rutecki, Grossman et al. 1989; Jones, Heinemmann et al. 1992; Pare, De Curtis et al. 1992; Nagao, Alonso et al. 1996).

Two populations of cells can be distinguished in the EC, based on their intrinsic electrophysiological properties: Stellate and non-stellate cells (Alonso and Klink 1993) . Stellate cells display a rythmic subthreshold oscillatory activity that is dependent on a persistent Na^+ conductance (Klink and Alonso 1993). Since it was our interest to characterize the nature of this conductance, we used the stellate cell population as a subject of study (see FIG 3B).

The Persistent Sodium Current (I_{NaP}) and its Role in Rythmicity.

The electrophysiological studies of EC layer II neurons have directly implicated them in the genesis of limbic network rythmicities (Alonso and Garcia-Austt 1987; Alonso and Llinas 1989; Alonso 1990). For example, field potential recordings show a characteristic theta rhythmicity (4-12 Hz) in the EC (Alonso and Garcia-Austt 1987). This

theta rhythm may be important for learning and memory (Gauthier, Destrade et al. 1982; Murray and Mishkin 1986; Greenstein, Pavlides et al. 1988; Doyere and Laroche 1992). A prominent theta activity is present in the hippocampus, the mammilary bodies, anterior thalamus and cingulate cortex (Leung and Borst 1987; Kocsis and Vertes 1994; Jahnsen and Llinas 1984). Up to date, the most widely accepted hypothesis for the generation of theta rhythm states that the medial septum of the basal forebrain acts as a "pacemaker" and that the rythmical firing of neurons in this nuclear structure drives "generators" in the hippocampus, the EC or other structures of the limbic system (Gaztelu and Buno 1982; Stewart and Fox 1990; Alonso et al 1996). However, recent electrophysiological evidence suggest that EC neurons have the intrinsic capability of generating subthreshold membrane potential oscillations that can contribute to theta and other rhythms (Konopacki, Golebiewski et al. 1992). Alonso and Llinas (Alonso and Llinas 1992) found that mammilary neurons possess an incredible autorhythmicity. Furthermore, these two authors demonstrated that I_{NaP} is necessary for the generation of "theta" rythmicity in single entorhinal layer II neurons (Alonso and Llinas 1989).

Given the close link between rythmicity and subthreshold oscillations, it is important to understand the mechanism for the generation of these oscillations. This is especially true for the EC "stellate cell" population, as it constitutes the main hippocampal input. In previous studies, Klink and Alonso (Klink and Alonso 1993) have postulated the existence of three currents that might be involved in subthreshold oscillatory behavior: I_H, a non-specific cationic current; I_K, a low threshold delayed rectifier; and I_{NaP}, a persistent Na^+ current. Initial work on the importance of I_{NaP} in oscillatory behavior was

performed by Alonso and Llinas (Alonso and Llinas 1989). They used single-electrode voltage clamp recordings to demonstrate that "theta-like" subthreshold oscillations in stellate cells were dependent on I_{NaP} activation. More recently, various researchers have investigated the origin of the persistent sodium current (Alzheimer et al 1993; Crill 1996; French et al 1990; Schwindt et al 1995; Stafstrom et al 1985; Ma, Catterall et al. 1996). Several hypothesis have been proposed for I_{NaP}. One hypothesis is that it represents a "window" current produced by the region of overlap between the inactivation and activation curves (FIG 5) (Hodgkin and Huxley 1952; Keynes 1994). An alternative hypothesis is that I_{NaP} is due to a subset of Na^+ channels with slowed or non-existant inactivation (Sugimori, Kay et al. 1994).

In the present study, we tested these two hypothesis for I_{NaP} in stellate cells using the whole-cell patch clamp technique on acutely dissociated neurons. The results of this work were presented at the 1996 meeting of the Society for Neuroscience (Galue and Alonso 1996) and will be part of a full paper.

Materials and Methods of the study

Tissue preparation

The brains of Long Evan male rats (90-110g) were removed following decapitation and placed immediately in iced-cold oxygenated Kreb's solution of the following composition (in mM): 124 NaCl, 5 KCl, 1.2 KH_2PO_4, 2.4 $CaCl_2$, 2.6 $MgSO_4$, 26 $NaHCO_3$, and 10 glucose. The pH of the Ringer's solution was maintained at 7.4 by saturation with 95% O_2- 5% CO_2. Horizontal brain slices of the retrohippocampal area were prepared as previously described (Alonso and Klink 1993). Briefly, horizontal slices

were cut at 500 μm using a vibratome and normally included the entorhinal cortex (medial and lateral), the hippocampal formation and part of the perirhinal cortex. Following sectioning, slices were incubated at room temperature in oxygenated Ringer solution for at least two hours before proceeding to the cell dissociation procedure. For dissociation, layer II of the medial EC was identified and dissected out. The piece of tissue (1.5 mm square) consisted of a dense band of cells that extends from the parasubiculum to the transition zone with the lateral EC as defined by Blackstad (Blackstad 1956). The tissue was incubated in a spinner flask filled with dissociation Ringer solution of the following composition (in mM): NaCl 115, KCl 5, PIPES 20 (from Sigma), $CaCl_2$ 1, $MgCl_2$ 4, glucose 25, and albumine 50mg/100ml. Proteinase K (from Sigma) was added to the gassed dissociation Ringer for 5 minutes at 30° +/- 3° C (mean +/- SE). Following several washouts, the tissue was treated for 30 minutes with Trypsine (1mg/ml from Sigma) previously dissolved in dissociation Ringer. Following this treatment, the slices were washed out and could be maintained for up to 7 hours (bubbled with 100% O_2). Prior to recording, the neurons were isolated by mechanical dissociation performed with fire polished *pasteur* pipettes. Cells obtained by dissociation varied in size and morphology. Healthy cells were recognized by their shiny appearance under phase-contrast optics (Kay 1989). During the dissociation procedure, the neurons lost most of their dendritic tree. However, the stellate cells were easily identifiable by their morphology which is clearly different from that of the pyramidal cells (Alonso and Klink 1993). Stellate cells displayed multiple primary dendrites whereas pyramidal cells had one or two major apical dendrites.

Recording

Patch electrodes were pulled from borosilicate glass and filled with a solution with the following composition (in mM): CsF 110, HEPES-(CsOH) 10, EGTA 11, $CaCl_2$ 1, $MgCl_2$ 2. The extracellular recording solution had the following composition (in mM): NaCl 100, TEA-Cl 40, HEPES Free acid 10, $CaCl_2$ 3, $MgCl_2$ 2, 4-AP 5. Cd^+ was added to the extracellular solution at concentration of 400μM to block Ca^{++} currents as well as Ca^{++} activated K^+ currents. Also, the electrodes were filled with Cs^+ to minimize contributions from K^+ currents.

Under visual control, the electrode tip was pressed against the surface of the cell and suction was applied to the electrode interior to form an electrode-cell membrane seal of several gigaohms' resistance. Further suction and hyperpolarization of the patch resulted in membrane rupture, giving low-resistance access to the cell interior. Electrode resistance was kept low (2-3 MΩ) in order to effectively clamp the sodium current. Filtering was 2KHz for ramps and 10KHz for pulses. Tetrodotoxin (TTX) was perfused by gravity flow to block Na^+ conductances.

Establishment and refining of the technique

In order to accomplish our objective of characterizing I_{Nap} using the voltage clamp approach, the technique of acute dissociation of neurons as well as the patch-clamp had to be set up. It was found that several details are critical for the stability of a recording while performing whole-cell voltage clamp in an acute dissociation preparation. First, it is important that the side of the recording camera be tilted in the place where the suction is

located. This tilting is essential to maintain a constant solution level in the camera even while changing solutions during the experiment. This constant level in the solution of the chamber is critical for the cell-pipette stability and quality of the patch. One lesson learned for future experiments is that a rectangular shaped camera is not ideal for rapid perfusion purposes. It took an average of 5 minutes for 300nM of TTX to block the currents. Because the quality of the experiment depends on how rapidly the procedure is completed, it is important to optimize the way drugs reach the cell. A perfusion system consisting on a round shaped recording chamber would be best for whole cell experiments in dissociated neurons, especially when drugs need to be applied.

It is also important to have some way of monitoring the level of suction applied to the cell while patching it. I found that visual control helps in the quality of the patch. Before applying suction, it was important that the pipette be lightly touching the cell membrane. Also, it was essential to be able to distinguish healthy from unhealthy cells. Healthy cells were the ones that showed no visible granules or nucleus when looked using the contrast optics. Bright, shiny cells with clear morphology and a gray dark elastic type of membrane were the best cells to patch.

Results

Activation

Voltage-dependent currents were recorded in acutely dissociated entorhinal cortex layer II neurons using whole-cell tight-seal voltage-clamp technique. I performed the study on 110 cells. Several criteria were chosen to judge the quality of the experiment. First, a high current to noise ratio when filtering at 10KHz and following a 2 second ramp

protocol had to be present. A typical current is shown in FIG 4. Second, the current baseline over the course of the experiment had to remain constant with respect to the initial value in control. Upon TTX perfusion, only a 2% variation of the baseline was allowed. This was the main criteria chosen to judge the stability and quality of the patch whose seals were usually greater than 2 GΩ (please refer to FIG 6). The cell had to remain stable for the complete experiment which included 7 different protocols: 1, 2, 4 and 8 second ramps, an inactivation protocol from -80mV, 100ms and 500ms step depolarization protocols for activation.

After screening of the acquired data, 15 neurons were chosen for the analysis of I_{Nap}. We examined the properties of I_{NaP} in a low Na^+ recording solution (see METHODS), by ramping the membrane potential from -80mV to +20mV at a rate of 0.1mV/mS (as shown in FIG 4). This rate was considered slow enough to inactivate I_{NaF} (Chao and Alzheimer 1995). To eliminate the possibility of contaminating currents, I_{NaP} was taken as the difference between current evoked at the same potential in the absence and presence of 300nM TTX (FIG 6) . Under these conditions we observed a TTX-sensitive current with a threshold between -63 and -60 mV.

I_{NaP} was not only quantified by means of ramp protocoles but also by using 500ms step depolarizations to different potentials. As shown in FIG 7, it can be seen that the Na^+ current increased in amplitude with membrane depolarization from approximately -60 to -35mV. In response to the step depolarizations, there was a relatively large, transient, inward current followed by a persistent inward current that became evident at about -60mV and reached maximum value at -34mV. Current-voltage relationships (IV's) were

obtained from the step depolarization measurements. FIG 8A shows the corresponding IV relationship for the ***persistent*** component of currents displayed in FIG 7. From these IV relations, a value for the reversal potential of the current was estimated. For the currents displayed in FIG 7, the reversal potential obtained by linear extrapolation between -25 and 0mV was 33 mV (see FIG 8A). This value was used to calculate activation curves, that then were fit with a Boltzman relation as described below. Currents were converted to conductance (g) for each cell, by using Omh's law: $g = I / E - E_r$, where E is the clamped membrane potential, E_r is the reversal potential obtained by linear extrapolation, and I is the recorded current. Conductances calculated from the persistent component of the currents displayed in FIG 7 are plotted against clamp potential in FIG 8B. The solid line through the data points is the Boltzman equation fit: $g = g_{max}/\{1+ \exp [(V_h-V)/k)]\}$ where g_{max} is the maximal conductance; V_h is the potential at which the conductance is half-maximal, and k is the slope factor. The g_{max}, V_h and k values for the curve in displayed in FIG 8B were 3.1 nS, -44mV, and 7.7 respectively. Table 1 displays the average values obtained for the 15 cells analyzed.

I also examined I_{NaF} in 8 stellate cells. FIG 9 shows a typical activation protocole used to study I_{NaF}. The family of currents were obtained by applying 5mV step depolarizations of 100ms in duration. The relationship of peak I_{NaF} as a function of test potential is displayed in FIG 10A. Activation curves for I_{NaF} were obtained in the same way as descibed for I_{NaP}. A typical example is displayed in FIG 10B. The average values obtained for the 8 cells analyzed are displayed in Table 1. I_{NaF} was found to activate always at more positive potentials than I_{NaP}.

Inactivation

The inactivation of the fast current was studied by examining the effects of varying levels of conditioning depolarization, on the amplitude of currents elicited by a subsequent test pulse. A 50ms test pulse to -20 mV was preceded by 100ms prepulses to 16 different depolarizing potentials starting at -80mV. The results obtained in a typical experiment are shown in FIG 11. The voltages indicated by the arrows correspond to the values of the ***prepulse potentials*** used to inactivate the current. The amplitude of the normalized peak current plotted against prepulse potential constitutes the inactivation curve displayed as open circles in FIG 11. The line through the points follows the equation: $I=I_{max}/\{1+\exp[(V- V_h)/k]\}$. The voltage for half-inactivation V_h was -63.9 mV. As mean of comparison, the plot also displays the activation curves for the fast and the persistent sodium currents of the same cell. It can be seen that the persistent current activates at more negative potentials than the fast current, in a region where window currents are not present. The average results obtained for the 7 cells analyzed, are displayed in Table 1.

Discussion

In the present study we characterized a persistent conductance present in layer II medial entorhinal cortex neurons. Previous work performed in our laboratory had implied the presence of this conductance and some of its parameters were measured using the current clamp technique (Klink and Alonso 1993). However, in order to appropriately characterize this conductance, especially its voltage dependence, a voltage clamp analysis was required.

Quite impressive I_{NaP} is observed in acutely dissociated entorhinal cells derived from either rat (Galue and Alonso 1996) or human brain tissue (Cummings, Xia et al. 1994) and typically measures between 50-500 pA in the rat. This represents about 5% of the peak Na^+ current. In its properties, the I_{NaP} characterized in the present study, is similar to other reported persistent sodium currents present in different parts of the central nervous system (Taylor 1993) . However, our studies disagree with previous reported results suggesting that I_{NaP} is a "window" current (Alzheimer, Schwindt et al. 1993; Brown, Schwindt et al. 1994). Window currents result from an overlap between the activation and inactivation curves of I_{NaF} . Two observations argue against a window current as a mechanism of I_{NaP} in the stellate cells of medial entorhinal cortex layer II. First, as shown in FIG 11, the activation curve of I_{NaP} occupies a more negative range of potentials than I_{NaF}. This observation suggests that I_{NaP} and I_{NaF} result form activation of a different set of channels with different voltages of activation. Second, we could detect this conductance at potentials more positive than expected for a "window" current. While these observations argue in favor of a specific noninactivating sodium current, we can not completely rule out the possibility that some of the persistant Na^+ currents in our experiments were dendritic currents that were poorly clamped. However, due to its large amplitude, its activation and inactivation profiles, and the quality of our acute dissociation, we believe that the persistent conductance present in the stellate cell population of the EC layer II neurons has a different origin than I_{NaF}.

The negative activation range of I_{NaP} is critical for its functional role in neurons (Jefferys 1990). Because I_{NaP} is activated about 10mV negative to spike threshold, it can add with synaptic currents. The subthreshold activation range of I_{NaP} is also critical for its ability to mediate the depolarizing phase of subthreshold membrane potential oscillations. Furthermore, the demonstrated presence of I_{NaP} in dendrites (Crill 1996) also helps in the amplification of distal synaptic excitation (Schwindt and Crill 1995). It has been shown that I_{NaP} can give rise to bursting activity and the formation of very robust paroximal-like depolarizations in entorhinal neurons (Klink and Alonso 1993), suggesting a contribution of I_{NaP} to epileptogenesis. Therefore, characterization of persistent currents and study of their modulation by neurotransmitters and pharmacological agents constitute an important step towards understanding epilepsy and its treatment.

PART TWO.

PHARMACOLOGY OF TYPE III NA^+ CHANNELS

Introduction

A growing body of evidence indicates that persistent Na^+ channels play a significant role in epileptogenesis. Direct evidence comes from studies that use electrophysiological recordings in solitary rat hippocampal neurons grown in microculture (Segal 1994). In that preparation, spontaneous ictus-like plateau depolarizations due to activation of a TTX-sensitive persistent Na^+ current, were frequently seen when calcium currents and glutaminergic transmission were suppressed. Neurons in epileptic foci, with a characteristic discharge pattern of rapid bursts of action potentials followed by interspike

intervals as brief as 2ms, have been described in human epileptic foci and in experimental animal models (Wyler et al). Intracellular recordings have shown that this pattern of discharge is generated by an abrupt, abnormal depolarization of neuronal membranes, which has been termed a "paroxysmal depolarization shift" or PDS (Matsumoto and Ajmone-Marsan 1964). Bursts similar to a PDS can be generated by the intrinsic membrane properties of the cell (Stafstrom et al 1984; Stafstrom, Schwindt et al. 1984). Therefore, the study of "persistent" depolarizations, their origin and pharmacological characterization, is an initial step towards the design of better anticonvulsant agents.

Persistent sodium channels may also be involved in chronic pain (Matzner and Devor 1994; Waxman, Kocsis et al. 1994). When peripheral nerves are damaged, they form a structure called a neuroma which is a source of chronic neuropathic pain (Devor 1994). Electrophysiological studies have shown that neuromas generate abnormal, spontaneous action potentials (Wall and Gutnick 1974). It has been proposed that persistent Na^+ currents contribute to the characteristic membrane depolarization that triggers these action potentials in the neuroma.

Sodium Channels and Anticonvulsant Action

Sodium channels are molecular targets for some of the most widely used anticonvulsant, antiarrhythmic and local anesthetic drugs, including phenytoin, carbamazepine and tetracaine (Catteral 1987; Butterworth and Strichartz 1990; Willow, Gonoi et al. 1985). It has been postulated that these drugs, although chemically diverse, may act at the same receptor site or at overlapping receptor sites on the channel protein (Ragsdale, McPhee et al. 1996). The drug receptor is believed to lie within the ion-

conducting pore (Ragsdale, McPhee et al. 1994) (see FIG 12), but its specific location has yet to be found.

Anticonvulsant and local anesthetic drugs inhibit brain Na^+ channels with complex voltage and activity-dependent properties (Starmer, Grant et al. 1984). Inhibition is weak when channels are activated from hyperpolarized holding potentials, but block becomes evident at more depolarized holding potentials (Ragsdale, Scheuer et al. 1991; Kuo and Bean 1994; Galue and Ragsdale 1997) (refer to FIG 13). The dependency of drug potency on membrane potential reflects the preferential drug binding to open and inactivated states of the channel which predominate at depolarized potentials, over resting states of the channel which predominate at hyperpolarized potentials (Cahalan 1980). The state-dependence of block can be explained by an allosterically-regulated drug receptor site that is in a low affinity conformation when channels are resting, and converts to a high affinity conformation when channels are open or inactivated (Rogawski and Porter 1990; McDonald and Kelly 1993). State-dependent block results in a selective inhibition of Na^+ currents during abnormal depolarization shifts (such as paroxysmal depolarization shifts, PDS) (Schwarz and Grigat 1989; Kuo, Chen et al. 1997) and during rapid trains of action potentials characteristic of abnormal cell activity such as those present in seizures. Persistent Na^+ currents have been proposed to contribute to the PDS. Pharmacological studies (Chao and Alzheimer 1995) have shown in fact that anticonvulsants such as phenytoin are very effective at inhibiting persistent currents in hippocampal neurons.

Pattern of Na^+ Channel Expression

The four sodium channel subtypes expressed primarily in brain neurons (Types I, II, III, VI) are differentially regulated during development in the central nervous system (Beckh, Noda et al. 1989). In the rat brain, Type III sodium channels appear first, reach peak mRNA levels late in embryonic life and decline to low levels by adulthood. Type III channels cause persistent currents (Jojo, Moorman et al. 1990; Galue and Ragsdale 1997) (see FIG 14) similar to those recorded in brain neurons (Cummings, Xia et al. 1994). Thus this channel is a molecular model to study I_{NaP} and its properties.

As the incidence of seizures is much higher in children than in adults, and pediatric seizure disorders are often unresponsive to conventional anticonvulsants (Shiner 1994), it is important to understand the mechanisms by which anticonvulsants exert their action on Na^+ channels expressed during development. Therapeutic agents that selectively inhibit persistent currents through Type III channels are likely to be particularly effective in treating childhood seizure disorders.

Type III channels may also be important for neuropathic pain. Studies using *in situ* hybridization show that its mRNA is selectively upregulated in dorsal root ganglion cells after peripheral nerve injury (Waxman, Kocsis et al. 1994). This abnormal expression of Type III channels may be one of the factors that contribute to abnormal action potentials in damaged nociceptive neurons. Despite the possible role of these channels in epilepsy and chronic pain, the action of anticonvulsant and local anesthetic drugs on them has not been investigated. Therefore, we performed an initial pharmacological characterization of

Type III channels by testing the action of some anticonvulsant and local anesthetic drugs when the channels are expressed alone, and when coexpressed with ß subunits . These results were presented at the 1997 Neuroscience meeting (Galue and Ragsdale, 1997) and are currently in preparation for submission as a full paper.

Materials and Methods of the Study

Functional Expression in Xenopus Oocytes

For oocyte expression studies, αIII, β1 and β2 cDNA's were subcloned into the plasmid vector pSP64T. This vector contains an SP6 promoter for *in vitro* RNA transcription and oocyte β-globin 5'-3'-untranslated sequences (including the poly (A) tract) which increase ion channel expression in oocytes . The pSP64T-BXN mRNA expression vector was used to generate mRNA suitable for injection into the oocytes. cRNA was transcribed from the pSP64T-BXN constructs using the comercially available mMessage Machine kit (Ambion). Synthesis was verified by spectrophotometric analysis and by gel electrophoresis. RNA was resuspended in 10mM Tris, 1mM EDTA pH 8.0 for injection into the oocytes. Oocytes were isolated from pieces of ovary obtained from female *Xenopus* frogs by treatment with collagenase and cultured in Barth's medium with the following composition in (mM): NaCl 88, KCl 1, $CaCl_2$ 0.41, $MgSO_4$ 0.82, $Ca(NO_3)_2$ 0.33, $NaHCO_3$ 2.4, HEPES 10 (from sigma), pH 7.4. Healthy stage 5-6 oocytes were pressure-injected with 50nl of wild Type α and ß subunits RNA.

Recording

The functional properties of the wild Type αIII sodium channel were examined 2 to 6 days after RNA injection, using the two-electrode voltage clamp recording technique. Pulses were applied and data acquired using an IBM PC and p-Clamp software (Axon Instruments). Capacity transients and series resistance were partially compensated using the internal clamp circuitry. Remaining transients and leak currents were substracted using the P/4 procedure (Bezanilla and Armstrong 1977). Microelectrodes were pulled from borosilicate glass and broken to a resistance of < 0.5 MΩ. They were filled with 3M KCl and shielded during recording to prevent capacitive coupling. Oocytes were continuously superfused with Ringer's solution with the following composition in (mM): NaCl 115, KCl 2.5, $CaCl_2$ 1.8, HEPES 10 (from sigma), pH 7.2 during recording. Drugs were applied through the superfusate. We examined the sensitivity of wild Type αIII sodium channels to the anticonvulsants phenytoin (Yaari, Selzer et al. 1986; Tunnicliff 1996), carbamazepine (Kuo, Chen et al. 1997; Schauf, Davis et al. 1974), and topiramate (Walker and Sander 1996; Zona, Ciotti et al. 1996). Also, we looked at the action of the anesthetic tetracaine (Butterworth and Strichartz 1990). Concentrations varied from 1 to 400 μM. Steady state inactivation was determined by giving prepulses to potentials ranging from -100 to -10 mV, followed by a test pulse to 0mV. The voltage dependence of block was assessed by varying the holding potential over a range from -100 to -30mV.

Results

Injection of oocytes with the rIII α subunit resulted in expression of functional Na^+ channels with slow inactivation properties as shown in FIG 14. Our initial experiments examined the effects of local anesthetics and anticonvulsant drugs on these currents using the two electrode voltage clamp recording technique.

Action of Phenytoin, Carbamazepine, Topiramate and Tetracaine on Sodium Channels Formed by rIII Alone.

Block by anticonvulsant and local anesthetic drugs is strongly dependent on membrane potential. To investigate the voltage-dependence of drug block, we started our experiments testing the effects of a given drug concentration on separate cells over a broad range of potentials. A slow inactivation protocol was applied to the cell. This consisted of a 10 second holding potential (HP) to 9 different depolarizing voltages, with each HP followed by a test pulse to 0 mV to elicit current. Upon termination of the protocol in control, the Na^+ current was allowed to recover at -90mV and then the drug was washed on. FIG 13 shows the action of 100μM phenytoin at different depolarizing potentials. It can be seen that current inhibition depends on the holding potential. The more depolarized the HP, the greater the amount of block. The data over a range of potentials was normalized with respect to the largest current in control and fit with a Boltzman equation of the form: $I = \{1/[1+\exp(X-V_h)/s]\}$, where I represents the current values normalized, X is the holding potential, V_h is the half inactivation voltage and s is the slope factor. An inactivation curve was obtained for each cell by plotting I values

against conditioning potential, both in control and in the presence of the drug. A typical example is shown in FIG 15A. It can be seen that the drug caused a negative shift in the voltage dependence of inactivation. From these inactivation curves, the voltage shift for half inactivation due to the presence of the drug was determined ($\Delta V_{1/2}$ in Table 2). Panel B shows the magnitude of $\Delta V_{1/2}$ over a range of phenytoin concentrations. We also examined the shift in half inactivation produced by carbamazepine, topiramate and tetracaine. As shown in panel C, carbamazepine displayed a similar degree of blocking effectiveness when compared to phenytoin. In contrast, topiramate caused only small shifts at very high drug concentrations. The local anesthetic tetracaine displayed a greater degree of blocking effectiveness when compared to phenytoin. A typical tetracaine experiment is shown in FIG 16.

We found that it was not possible to perform complete inactivation curves in the same cell over a broad range of drug concentrations because Type III channels exhibit an irreversible run down in current amplitude with repeated long depolarizations. To counteract the build up of inactivation over the time course of the experiment, we decided to perform complete dose response experiments on the same cell using a limited number of holding potentials: -100, -70 and -40 mV. The blocking effect of phenytoin and carbamazepine was highly dependent on holding potential as shown in the dose response curves displayed in FIG 17. At very hyperpolarized potentials such as -100mV, high concentrations of phenytoin (up to 200μM) exerted modest block of the Na^+ current. At more depolarized potentials where Na^+ current inactivation is present,

phenytoin had a stronger blocking action. The data displayed in FIG 17 were fitted by the one to one binding curve: y= {1/(1+[Phenytoin]/K)}, where K is the concentration that gives 50% block. Average K values obtained for all the experiments are displayed as a bar graph in FIG 18. The highest affinity of block occurred at a holding potential of -40mV, where the Na^+ current was inactivated in a range between 50 and 80%. At that potential, phenytoin blocked the current with a K value of 136μM. The weakest block occurred at -100 mV where inactivation was less than 5%. The K value obtained for phenytoin at -100mV was 991μM. Topiramate concentrations as high as 2mM exerted virtually no block of the rIII currents as shown in FIG 17.

rIIIß$_1$ß$_2$ and rII Channels.

Functional sodium channels in the mammalian brain are a heterotrimer, formed by the association of α with two auxiliary *ß* subunits (Catteral 1995). Both $ß_1$ and $ß_2$ subunits have been shown to modulate Na^+ channel activity (Isom, De Jong et al. 1992; Isom, Scheuer et al. 1995; Meadows, Seltzer et al. 1997). Indeed, both subunits shift the half voltage of activation to more hyperpolarized potentials and alter the channel kinetics by accelerating both, activation and inactivation processes (Meadows, Seltzer et al. 1997). Given the important modulatory actions that these subunits have on channel function, we wanted to test how anticonvulsant and local anesthetic action was altered with coexpression of these subunits with αIII. For comparison, we performed the same kinds of experiments using the ***rIIA*** channel, a major isoform in the adult rat brain (Brysch, Creutzfeldt et al. 1991). When expressed alone in oocytes ***rIIA*** forms slow gating channels, but when it is coexpressed with $ß_1$ and $ß_2$, it forms rapidly inactivating channels. In contrast, coexpression of the auxiliary subunits with rIII results in currents that rise more rapidly to a peak, but still inactivate slowly. Previous studies have shown that anticonvulsants and local anesthetics have strong effects on rIIA currents (Ragsdale, Scheuer et al. 1991). Taking this into consideration, we decided to use the rIIA channel as a way to compare the results obtained with the rIII slow inactivating type of channel. Complete dose response experiments were performed on these two types of channels. The data were fitted following the same method described for the rIII channel. K values are displayed in Table 4. The results suggest that rIIA is considerably more sensitive to

phenytoin than rIII at depolarized potentials. However for carbamazepine, tetracaine and topiramate, there is no clear difference between these two channel subtypes.

Functional Considerations

In human and other mammals, development is characterized by an increased susceptibility to seizures. This may be due, at least in part, to the functional properties of the membrane ion channels that are expressed in developing brain neurons. It is known that in immature rat brain, the Type III channels cause persistent currents that are likely to increase neuronal excitability and therefore contribute to epileptogenesis. As predicted, the anticonvulsant drugs tested in the present study have strong effects on these persistent currents. However, in contrast to our expectations, fast inactivating sodium currents exhibited similar sensitivities to the agents tested when compared with the slow inactivating type. This could indicate that for both types of channels, the receptor site is located in similar locations. Based on previous work, Ragsdale et al.1996 have proposed that highly conserved residues in the IVS6 transmembrane segment of the sodium channel α subunit form part of the anticonvulsant/local anesthetic receptor site. It is likely that the anticonvulsant/local anesthetic receptor site is formed by multiple regions of the channel protein in addition to those already postulated. It would be interesting to test the Type III channel for additional determinants of drug action, and to use site-directed mutagenesis to study with precision the inactivation loop region of the channel and its relation with drug action.

With respect to the topiramate studies, it would appear that its action is not mediated via Type III channel block. The molecular basis of topiramate's action is not

known. It has been proposed to interact with excitatory amino acid receptors (Coulter et al. 1993), GABAergic responses (Brown at al. 1993) and voltage-gated sodium channels. The evidence for interaction with sodium channel includes inhibition of sustained repetitive firing in cultured hippocampal neurons (Coulter et al 1993) and voltage-dependent inhibition of sodium currents in voltage-clamp recordings from cultured cerebellar granule cells (Zona et al 1996). It might be the case that repetitive firing in these neurons is mediated via persistent Na^+ currents that mechanistically differ from those produced by Type III channels. As suggested in the introductory part of the present work, high frequency repetitive firing can be "sustained" by persistent Na^+ currents that result from fast inactivating Na^+ channel modal gating and ***not*** by persistent currents resulting from activation of a different set of Na^+ channel subtype.

CONCLUSION

This study has investigated persistent sodium currents using two approaches: Voltage-clamp recording using acutely dissociated neurons from rat brain cortex, and two-electrode voltage clamp analysis using the *oocyte* expression system.

The work presented here had two main findings: the first was the fact that medial entorhinal cortex layer II stellate neurons do indeed possess a persistent sodium conductance (I_{NaP}) that activates 10 mV more negative than the transient sodium conductance (I_{NaF}). This property allows I_{Nap} to sustain the oscillatory behavior characteristic of the layer II stellate population in the entorhinal cortex. The second was that the rIII channel expressed in *Xenopus* oocytes constitutes a good molecular model to study persistent currents. Indeed, we demonstrated that this channel is sensitive to local anesthetic and anticonvulsant drugs. An insight about the specificity of the interaction between these drugs and the receptor site in the channel was also obtained. Topiramate, a blocker of Na^+ currents in brain neurons, had almost no effect blocking the persistent conductance generated by the rIII channel.

Given the important role that persistent currents play in normal brain activities such as rythmicity, as well as in pathological states such as epilepsy and pain, their study offers new insights about brain function and provides cues for new pharmacological developments.

REFERENCES

Alonso, A., De Curtis,M., and Llinas, R (1990). "Postsynaptic hebbian and non-hebbian long-term potentiation of synaptic efficacy in the entorhinal cortex in slices and in the isolated adult guinea pig brain." Proc. Natl.Acad.Sci(87): 9280-9284.

Alonso, A. et al (1996). "Differential oscillatory properties of cholinergic and non-cholinergic nucleus basalis neurons in guinea pig brain slice." Eur. J. Neurosci **8**: 169-182.

Alonso, A. and E. Garcia-Austt (1987). "Neuronal sources of theta rhythm in the entorhinal cortex of the rat. II Phase relations between unit discharges and theta field potentials." Expl Brain Res **67**: 502-509.

Alonso, A. and E. Garcia-Austt (1987). "Neuronal sources of theta rhythm in the entorhinal cortex. I Laminar distribution of theta field potentials." Exp. Brain. Res. **67**(493-501).

Alonso, A. and R. Klink (1993). "Differential electroresponsiveness of stellate and pyramidal-like cells of medial entorhinal cortex layer II neurons." J.Neurophysiol. **70**: 128-143.

Alonso, A. and R. Llinas (1989). "Subthreshold Na+ - dependent theta-like rhytmicity in stellate cells of entorhinal cortex layer II neurons." Nature **342**: 175-177.

Alonso, A. and R. R. Llinas (1992). "Electrophysiology of the mammillary complex in vitro. II. Medial mammillary neurons." J. Neurophysiology **68**: 1321-1331.

Alzheimer, C., P. C. Schwindt, et al. (1993). "Modal gating of Na+ channels as a mechanism of Persistent Na+ current in pyramidal neurons from rat and cat sensorimotor cortex." J Neurosci. **13**: 660-673.

Amaral, D. G. and R. Insausti (1990). The human hippocampal formation. The Human Nervous system. G. Paxinos. New York, Academic Press.

Beckh, S., M. Noda, et al. (1989). "Differential regulation of three sodium channel mRNAs in the rat central nervous system during development." The Embo Journal **8**(12): 3611-3616.

Bezanilla, F. and C. M. Armstrong (1977). "Inactivation of the Sodium channel. I Sodium current experiments." Journal of General Physiology **70**: 549-566.

Blackstad, T. W. (1956). "Commisural connections of the hippocampal region in the rat, with special reference to their mode of termination." J. Comp. Neurol **105**: 417-521.

Brown, A. M., P. C. Schwindt, et al. (1994). "Different voltage dependence of transient and persistent Na currents is compatible with modal-gating hypothesis for Na channels." J of Neurophysiology 71(6): 2562-2565.

Brown, S.D., Wolf, H.H et al. (1993). "The novel anticonvulsant topiramate enhances GABA-mediated chloride flux". Epilepsia **34** (Suppl./* 2) s122-s125

Brysch, W., O. D. Creutzfeldt, et al. (1991). "Regional and temporal expression of sodium channel messenger RNAs in the rat brain during development." Exp Brain Res **86**: 562-567.

Butterworth, J. F. and G. R. Strichartz (1990). "Molecular mechanisms of local anesthesia: A review." Anesthesiology 72: 711-734.

Cahalan, M., Shapiro, B., Almers, W (1980). "Relationship between inactivation of sodium channels and block by quaternary derivatives of local anesthetics and other compounds". Molecular mechanisms of anesthesia, Progress in anesthesiology **2**: 17-33

Catteral, W. A. (1987). "Common modes of drug action on Na channels: local anesthetics, antiarrhythmics and anticonvulsants." Tips Reviews **8**: 57-65.

Catteral, W. A. (1992). "Cellular and molecular biology of voltage gated sodium channels." Physiol.Rev 72(Suppl): s15-s46.

Catteral, W. A. (1995). "Structure and function of voltage-gated ion channels." Annu.Rev.Biochem. **64**: 493-531.

Chao, I. T. and C. Alzheimer (1995). "Effects of phenytoin on the persistent NA current of mammalian CNS neurons." Neuroreport **6**(13): 1778-1780.

Chao, T. I. and C. Alzheimer (1995). "Do neurons from rat neostriatum express both a TTX-sensitive and a TTX-insensitive slow Na current ?" J of Neurophysiology **74**: 934-941.

Crill, W. E. (1996). "Persistent sodium current in mammalian central neurons." Annu.Rev.Physiol **58**: 349-362.

Cummings, T. R., Y. Xia, et al. (1994). "Functional properties of rat and human neocortical voltage-sensitive sodium currents." J. Neurophysiology **71**: 1052-1064.

Dasheiff, R. M. and J. O. McNamara (1982). "Electrolitic entorhinal lesions cause seizures." Brain Res **231**: 444-450.

Devor, M. (1994). The pathophysiology of damaged peripheral nerves. Texbook of pain. P. D. Wall and R. Melzack. Edinburg, Churchill Livingston: 79-100.

Doyere, V. and S. Laroche (1992). "Linear relationship between the maintenance of hippocampal long term potentiation and retention of an associative memory." Hippocampus **2**: 39-48.

French , C.R., Sah, P., Buckett, K.J., Gage, P (1990). "A voltage-dependent persistent sodium current in mammalian hippocampal neurons. J. of Gen Physiol **95**: 1139-1157

Galue, A. M. and A. Alonso (1996). "Properties of the persistent Na current generating subthreshold oscillations in entorhinal cortex (EC) layer II neurons." Soc. Neurosci. Abstr **22**: 61.

Galue, A. M. and D. S. Ragsdale (1997). "Inhibition of rat brain Type III sodium channels by local anesthetic and anticonvulsant drugs." Soc. Neurosci. Abstr **23**: 1475.

Gauthier, M., C. Destrade, et al. (1982). "Late post-learning participation of entorhinal cortex in memory processes." Brain Res **233**: 255-264.

Gaztelu, J. M. and W. Buno (1982). "Septo-hippocampal relationships during EEG theta rhytm." Electroencephalogr. Clin.Neurophysiol **54**: 375-387.

Gomez-Isla, T., J. L. Price, et al. (1996). "Profound loss of layer II entorhinal cortex neurons occurs in very mild Alzheimer's disease." J. of Neuroscience **16**: 4491-4500.

Gonoi, T. and B. Hille (1987). "Gating of Na channels." J. Gen. Physiol **89**: 253-274.

Greenstein, Y. J., C. Pavlides, et al. (1988). "Long term potentiation in the dentate gyrus is preferentially induced at theta rhythm periodicity." Brain Res **438**: 331-334.

Hauser, W. A. (1994). Epilepsia **35**(Supplem): S1-S6.

Hodgkin, A. L. and A. F. Huxley (1952). "A quantitative description of membrane current and its application to conduction and excitation in nerve." J. Physiol (Lon.) **117**: 500-544.

Hyman, B. T., G. W. Van Hoesen, et al. (1986)a. "Perforant pathway changes and the memory impairment of Alzheimer's disease." Ann. Neurol. **20**: 472-481.

Hyman, B. T., G. W. Van Hoesen, et al. (1986)b. "Alzheimer's DIsease: Cell-specific pathology isolates the hippocampal formation." Science **225**: 1168-1170.

Hyman, B. T., G. W. Van Hosen, et al. (1990). "Memory-related neural system in Alzheimer's disease : An anatomic study." Neurology **40**: 1721-1730.

Isom, L. L., K. S. De Jong, et al. (1992). "Primary structure and functional expression of the B1 subunit of the rat brain sodium channel." Science **256**: 839-842.

Isom, L. L., T. Scheuer, et al. (1995). "Functional co-expression of the B1 and Type II A alpha subunits of sodium channels in a mammalian cell line." J Biol Chem **270**: 3306-3312.

Jahnsen, H. and R. R. Llinas (1984). "Ionic basis for the electroresponsiveness and oscillatory properties of guinea-pig thalamic neurons in vitro." J. Physiol **349**: 227-247.

Jefferys, J. G. R. (1990). "Intrinsic burst mechanisms and the paroximal depolarization shift (PDS) in: Basic mechanisms of focal epilepsies." Experimental Physiology **75**: 127-162.

Jojo, R. H., J. R. Moorman, et al. (1990). "Toxic and kinetic profile of rat brain Type III sodium channels expressed in Xenopus oocytes." Mol. Brain Res 7: 105-113.

Jones, R. S. G. (1993). "Entorhinal-hippocampal connections: a speculative view of their function." Trends Neurosci **16**: 58-64.

Jones, R. S. G., U. F. H. Heinemmann, et al. (1992). The entorhinal cortex and generation of seizure activity: Studies of normal synaptic transmission and epileptogenesis Neurotransmitters in Epilepsy. Neurotransmitters in Epilepsy. A. G. Amsterdam, Elsevier: 173-180.

Kay, A. R. (1989). A procedure for isolating neurons from the mature mammalian brain. A dissection and tissue culture manual of the nervous system. A. Shahar, J. d. Vellis and A. Vernadakis. New York, Alan R. Liss, Inc.

Keynes, R. (1994). "Bimodal gating of the Na channel." Trends Neurosc **17**(2): 58-61.

Klink, R. and A. Alonso (1993). "Ionic Mechanisms for the subthreshold oscillations and differential electroresponsiveness of medial entorhinal cortex layer II neurons." J. of Neurophysiology **70**: 144-157.

Kocsis, B. and R. P. Vertes (1994). "Characterization of neurons in the supramammillary nucleus and mammillary body that discharge rhytmically with the hippocampal theta rhythm in the rat." J. Neurosci **14**: 7040-7052.

Konopacki, J., H. Golebiewski, et al. (1992). "Carbachol - induced theta-like activity in entorhinal cortex slices." Brain Res **572**: 76-90.

Krieg, L. and P. Pelton (1984). .

Kuo, C. C. and B. Bean (1994). "Slow binding of phenytoin to inactivated sodium channels in rat hippocampal neurons." Mol Pharmacol **46**: 716-725.

Kuo, C. C., R. S. Chen, et al. (1997). "Carbamazepine inhibition of neuronal Na currents: Quantitative distinction from phenytoin and possible therapeutic implications." Molecular Pharmacology **51**: 1077-1083.

Leung, L. W. S. and J. G. G. Borst (1987). "Electrical activity of the cigulate cortex. I. Generating mechanisms and relations to behavior." Brain Res **407**: 68-80.

Llinas, R. R. (1988). "The intrinsic elecrtrophysiological properties of mammalian neurons: Insights into central nervous system function." Science **242**: 1654-1664.

Lorente de No, R. (1933). "Studies on the structure of the cerebral cortex. I The area entorhinalis." J. Psychol. Neurol. **45**: 381-438.

Ma, J. Y., W. A. Catterall, et al. (1996). "Induction of persistent Na current by overexpression of G-protein BG subunits." Soc. Neurosci. Abstr **22**: 57.

Matsuki , N., Quandt, F.N., et al (1983) "Characterization of the block of sodium channels by phenytoin in mouse neuroblastoma cells". J of pharmacology and experimental therapeutics **228** (2): 523-530

Matsumoto, H. and C. Ajmone-Marsan (1964). "Cortical cellular phenomena in experimental epilepsy: Ictal manifestations." Exp. Neurol **9**: 305-326.

Matzner, O. and M. Devor (1994). "Hyperexcitability at sites of nerve injury depends on voltage sensitive Na channels." J of Neurophysiology **72**: 350-359.

McDonald, R. L. and K. M. Kelly (1993). "Antiepileptic drug mechanisms of action." Epilepsia **34**(Suppl 5): S1-S8.

Meadows, L., A. Seltzer, et al. (1997). "Modulation of slowly gating embryonic sodium channel by auxiliary B1, B1A and B2 subunits." Submitted for publication.

Murray, E. A. and M. Mishkin (1986). "Visual recognition in monkeys following rhinal cortical ablations combined with either amigdalectomy or hippocampectomy." J Neurosc **6**: 1991-2003.

Nagao, T., A. Alonso, et al. (1996). "Epileptoform activity induced by pilocarpine in the rat hippocampal-entorhinal slice preparation." Neuroscience **72**: 399-408.

Pare, D., M. De Curtis, et al. (1992). "Role of the hippocampal-entorhinal loop in temporal lobe epilepsy: extra and intracellular study in the isolated guinea-pig brain in vitro." J of Neurosc **12**: 1867-1881.

Patlak, J. (1991). "Molecular kinetics of Voltage-dependent Na channels." Physiological reviews **71**(4): 1047-1080.

Ragsdale, D. R., J. C. McPhee, et al. (1996). "Common molecular determinants of local anesthetic, antiarrythmic, and anticonvulsant block of voltage-gated Na channels." Proc.Natl.Acad.Sci.USA **93**: 9270-9275.

Ragsdale, D. S., J. C. McPhee, et al. (1994). "Molecular determinants of state-dependent block of Na+ channels by local anesthetics." Science **265**: 1724-1728.

Ragsdale, D. S., T. Scheuer, et al. (1991). "Frequency and voltage-dependent inhibition of Type IIA Na+ channels, expressed in a mammalian cell line, by local anesthetic, antiarrythmic, and anticonvulsant drugs." Mol.Pharmacol **40**: 756-765.

Ramon y Cajal, S. (1911). Histologie du Systeme Nerveux de l'Homme et des Vertebres. Paris.

Rogawski, M. A. and R. Porter (1990). "Antiepileptic Drugs: Pharmacological mechanisms and clinical efficacy with consideration of promising developmental stage compounds." Pharmacological reviews **42**(3): 223-286.

Rutecki, P. A., R. G. Grossman, et al. (1989). "Electrophysiological connections between the hippocampus and entorhinal cortex in patients with complex partial seizures." J. Neurosurg. **70**: 667-675.

Ruth, R. E., T. E. Collier, et al. (1982). "Topography between the entorhinal cortex and the dentate septotemporal axis of the dentate gyrus in rats. I. Medial and intermediate entorhinal projecting cells." J. comp. Neurol **209**: 69-78.

Schauf, C. L., F. A. Davis, et al. (1974). "Effects of carbamazepine on the ionic conductances of Myxicola giant axons." J of Pharmacol. Exp. Ther **189**(538-543).

Schwarz, J. R. and G. Grigat (1989). "Phenytoin and carbamazepine: Potential and frequency - dependent block of Na currents in mammalian myelinated nerve fibers." Epilepsia **30**(3): 286-294.

Schwindt, P. C. and W. E. Crill (1995). "Amplification of synaptic current by persistent sodium conductance in apical dendrite of neocortical neurons." J Neurophysiology **74**: 2220-2224.

Segal, M. M. (1994). "Endogenous bursts underlie seizurelike activity in solitary excitatory hippocampal neurons in microcultures." J.Neurophysiol **72**: 1874-1884.

Shinner, S (1994). "Discontinuing antiepileptic drugs in children with epilepsy: a prospective study". Annals of Neurology **35 (5)**: 534-45.

Stafstrom, C. E. et al (1984). "Properties of subthreshold response and action potential recorded in layer V neurons from cat sensorimotor cortex in vitro." J Neurophysiology **52**: 244-263.

Stafstrom, C. E., P. C. Schwindt, et al. (1984). "Repetitive firing in layer V neurons from cat neocortex in vitro." J. Neurophysiology **52**: 264-277.

Stafstrom, C.E., Schwindt, P.C., Chubb, M., Crill, W.E (1985). "Properties of persistent sodium conductance and calcium conductance of layer V neurons from cat sensorimotor cortex in vitro". J. of Neurophysiology **52:** 264-277

Starmer, F. C., A. O. Grant, et al. (1984). "Mechanisms of use-dependent block of sodium channels in excitable membranes by local anesthetics." Biophysical Journal **46**: 15-27.

Steward, O. (1976). "Topographic organization of the projections from the entorhinal area to the hippocampal formation in the rat." J. com. Neurol **167**: 285-314.

Steward, O. and S. A. Scoville (1976). "The cells of origin of entorhinal afferents to the hippocampus and fascia dentata of the rat." J. com. neurol **169**: 347-370.

Stewart, M. and S. E. Fox (1990). "Do septal neurons pace the hippocampal theta rhythm?" Trends Neurosci **13**: 163-168.

Stuhmer, W., F. Conti, et al. (1989). "Structural parts involved in activation and inactivation of the sodium channel." Nature **339**: 597-603.

Sugimori, M., A. R. Kay, et al. (1994). "The persistent Na current in cerebellar purkinje cells has a single channel conductance distinct from the inactivating current." Soc. Neurosc. Abstr **20**: 63.

Taylor, C. P. (1993). "Na currents that fail to inactivate." Trends Neurosc. **16**: 455-460.

Tunnicliff, G. (1996). "Basis of antiseizure action of phenytoin." Gen Pharmac **27**(7): 1091-1097.

Van Hoesen, G. W., Hyman B.T., and Damasio A.R (1991). "Entorhinal Cortex Pathology in Alzheimer's disease." Hippocampus **1**(1): 1-8.

Walker, M. C. and J. W. A. S. Sander (1996). "Topiramate: a new antiepileptic drug for refractory epilepsy." Seizure **5**: 199-203.

Wall, P. D. and M. Gutnick (1974). "Properties of afferent nerve impulses originating from a neuroma." Nature (London) **248**: 740-743.

Waxman, S. G., D. Kocsis, et al. (1994). "Type III Sodium Channel mRNA is expressed in embryonic But not Adult Spinal Sensory Neurons, and is Reexpressed Following Axotomy." J of Neurophysiology **72**(1): 466-468.

Willow, M., T. Gonoi, et al. (1985). "Voltage clamp analysis of the inhibitory actions of diphenylhydantoin and carbamazepine on voltage-sensitive sodium channels in neuroblastoma cells." Molecular pharmacology **27**: 549-558.

Wyler, A., Ojemann, G.A and Ward, A.A (1982). "Neurons in human epileptic cortex: correlation between unit and EEG activity." Annals of Neurology **11**(3): 301-308.
Yaari, Y., M. Selzer, et al. (1986). "Phenytoin: Mechanisms of its anticonvulsant action." Ann Neurol **20**: 171-184.

Zona, C., M. T. Ciotti, et al. (1996). "Topiramate attenuates voltage-gated sodium currents in rat cerebellar granule cells." J of Neurophysiology **74** (1): 364-368.

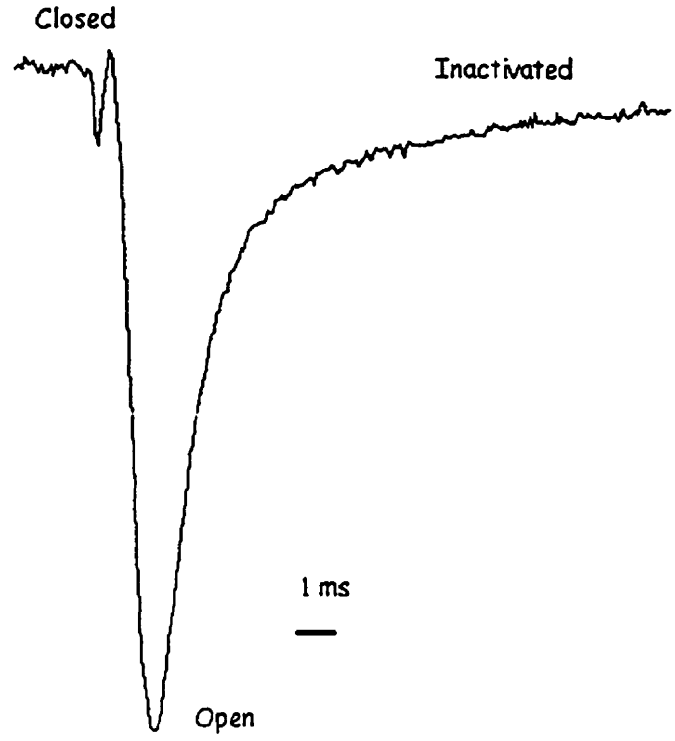

FIG. 1.

Fast sodium current recorded from a rat entorhinal neuron. 80% of inactivation occurs within 3 ms. The current is in response to a depolarizing pulse to 0mV from a resting membrane potential of -80mV. Most of the currents recorded were 5-10 nA in amplitude.

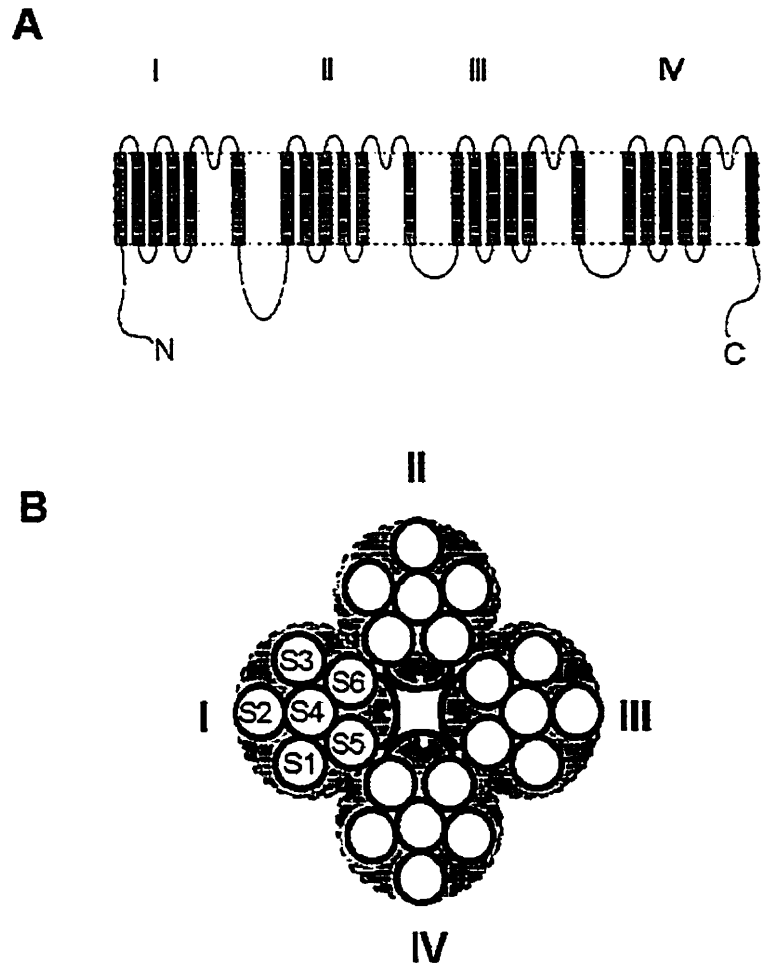

FIG. 2.

Diagramatic representation of the sodium channel α subunit.
A. Each rectangle represents a transmembrane alpha helix. When the three dimensional structure of the channel is looked at from above, one obtains figure B.

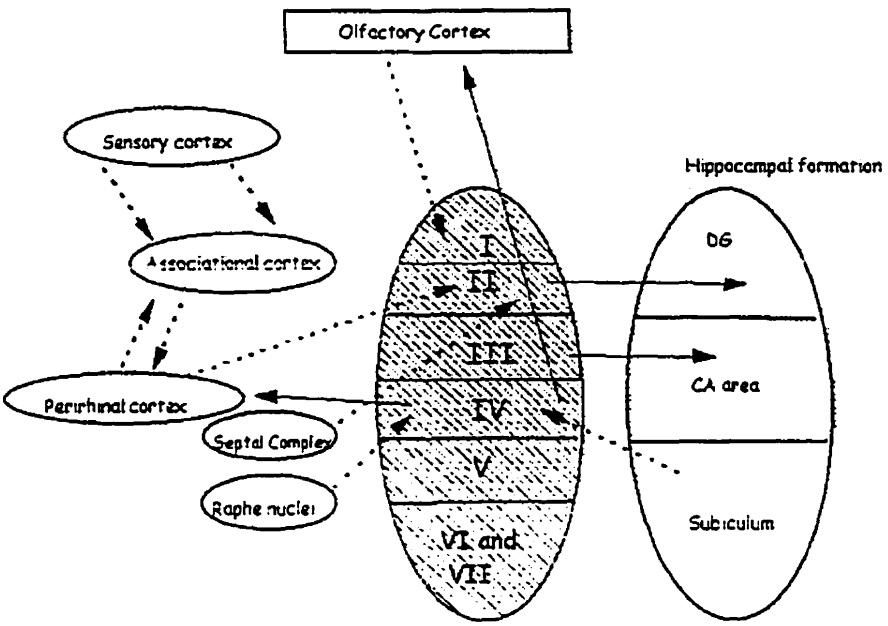

FIG. 3.A

Main connections of the entorhinal cortex (shown as a shadow area). Information flows from several cortical areas into the enthorinal cortex. This structure then sends projections to the hippocampal formation. The information returns to the entorhinal area which then projects back to other regions of the cortex. Among subcortical inputs, only those coming from the septal and raphe nuclei are displayed.

FIG 3B.
Morphology of a medial entorhinal cortex layer II Stellate cell. The cell was injected with biocytine after intracellular recording was performed.
The cell body is approximately 10μm in diameter.

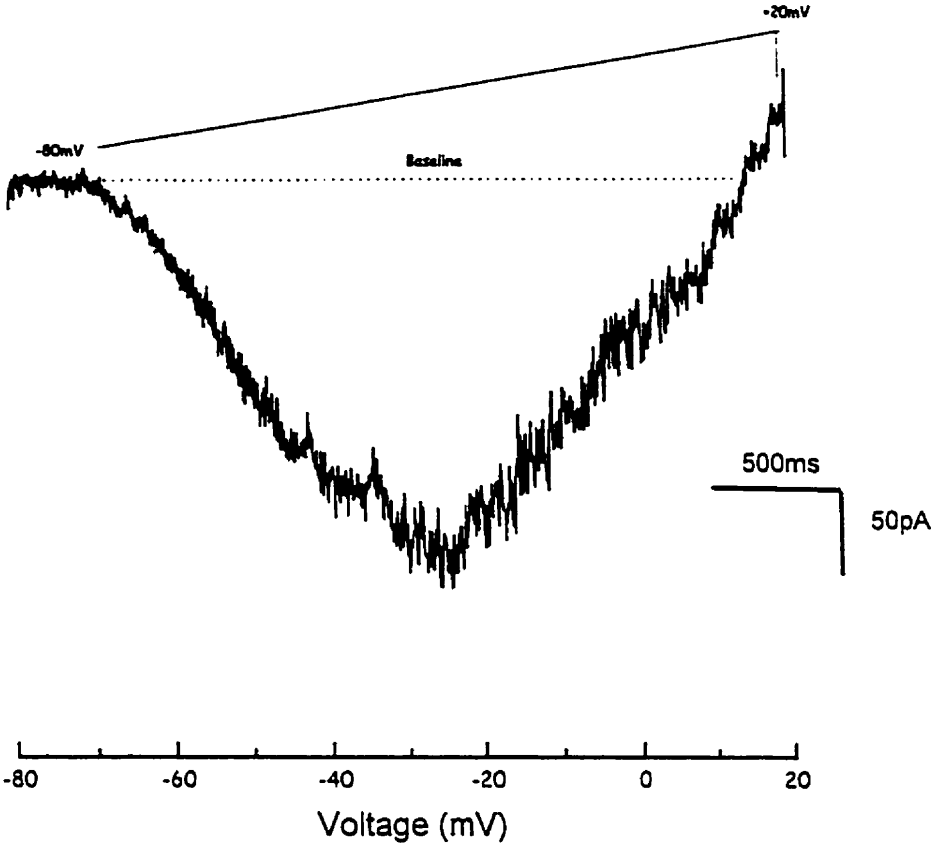

FIG 4.

Persistent sodium current (I_{Nap}) recorded in a stellate cell. The 200pA current resulted when a gradual depolarization was applied from a resting membrane potential of –80mV. The protocole displayed is a 2 sec ramp depolarization (0.1mV/ms). TTX has been substracted and the resultant Na^+ current activates at approximately –65mV.

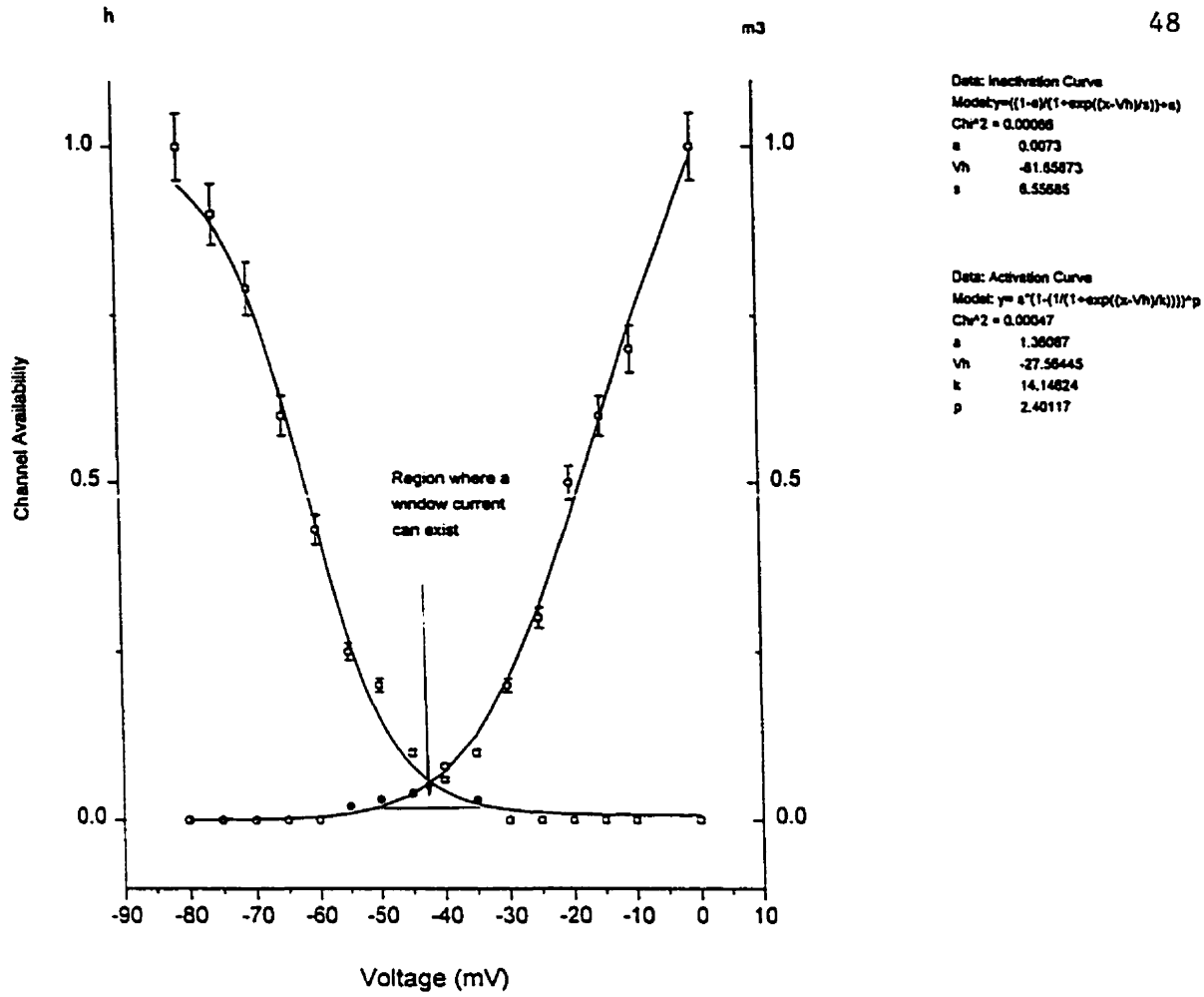

FIG 5.

Activation and Inactivation curves for the fast sodium current (I_{NaF}) of a stellate cell. The points are the average of 8 experiments. Window currents are expected between –60 and –30mV. The data were fitted with the Boltzman distribution as described in the text.

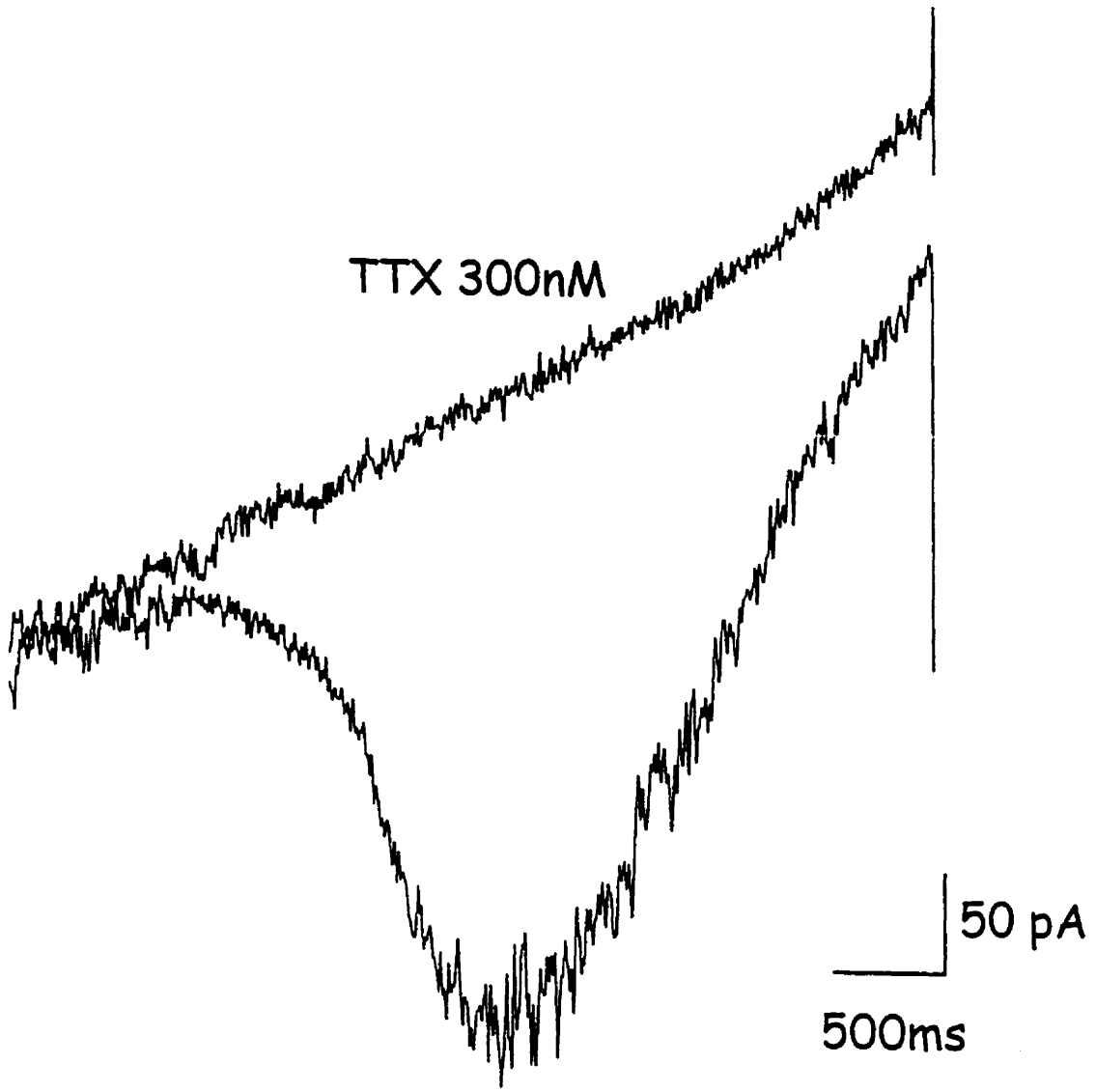

FIG. 6.

Perfusion of 300nM TTX for 4 minutes, completely abolished the persistent Na^+ current.

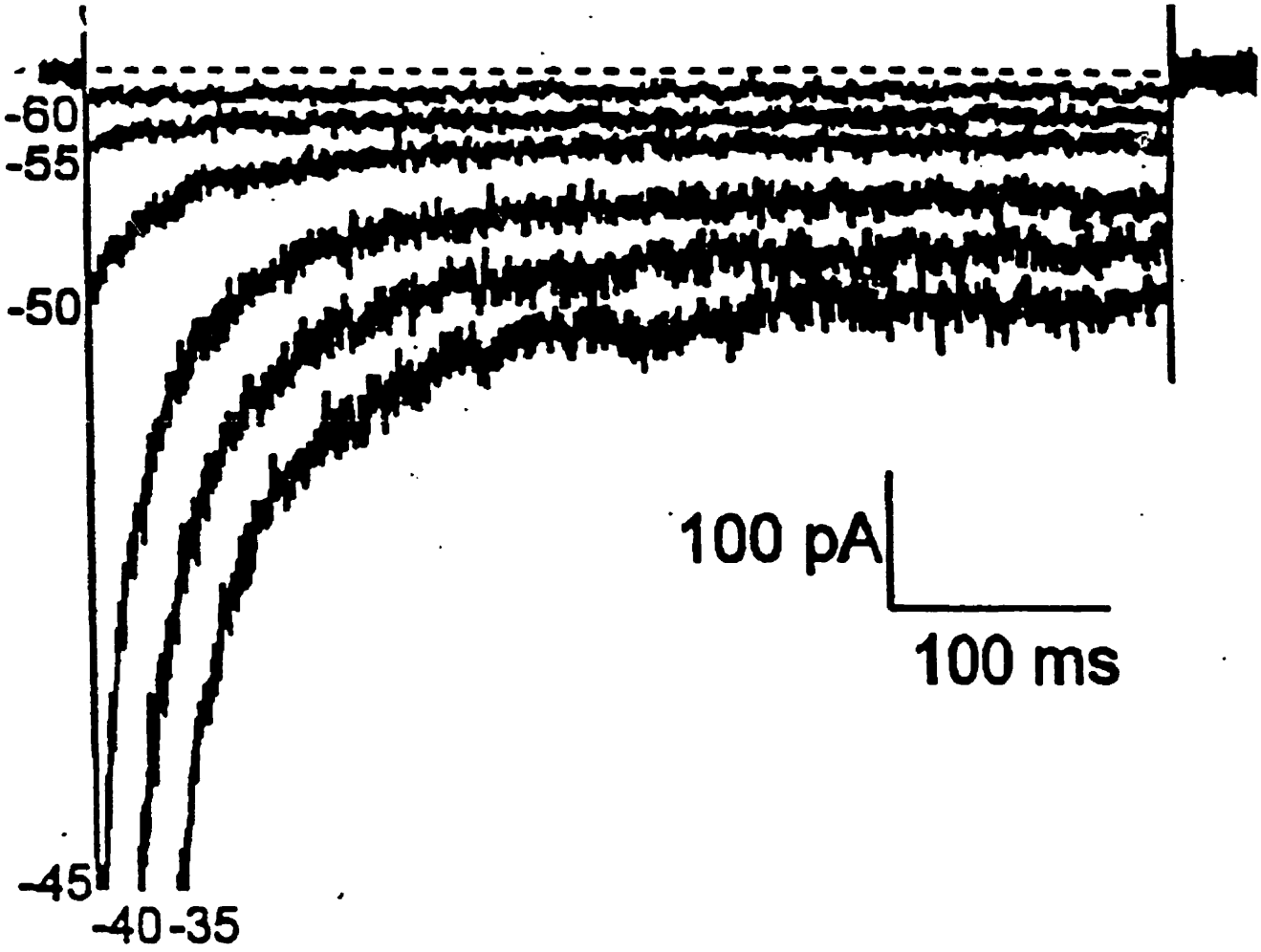

FIG. 7.

Current evoked by 500mS long step depolarization in 5mV increments. Maximal current amplitudes were observed at -35mV. The figure displays both, the transient and the persistent components of the Na^+ current; however at -45, -40, and -35 mV the peaks of the transient currents are clipped because of the large amplitude.

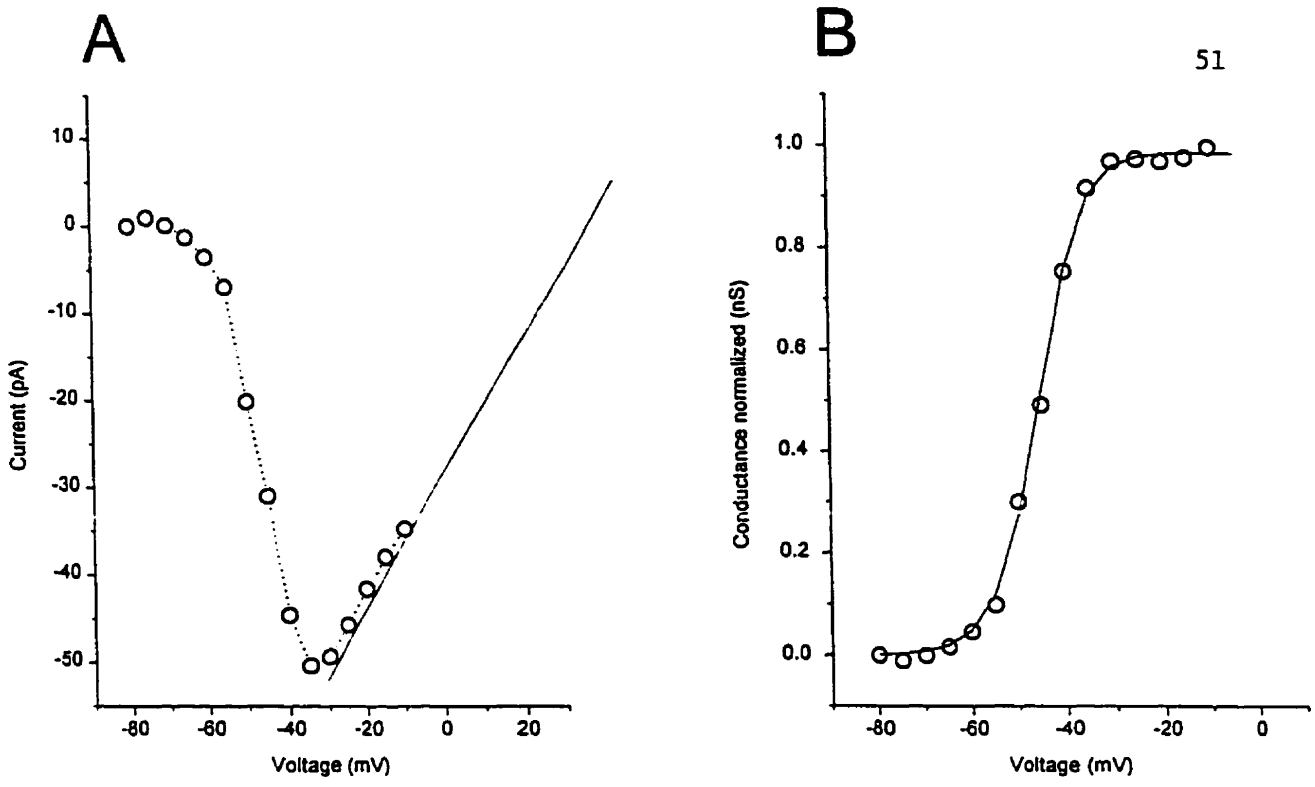

FIG. 8
A. Current-voltage relationship of the current displayed in FIG 7.
B. Activation curve obtained from the current-voltage relationship displayed in panel A.

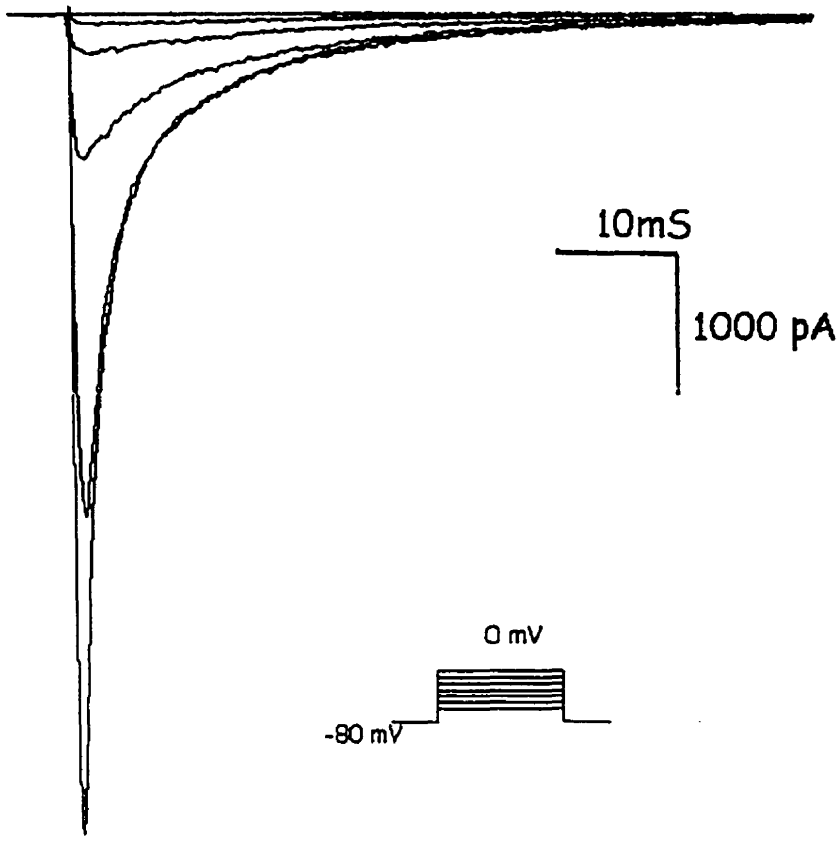

FIG. 9.

Transient sodium current evoked by 100mS long depolarizations in 5mV increments.

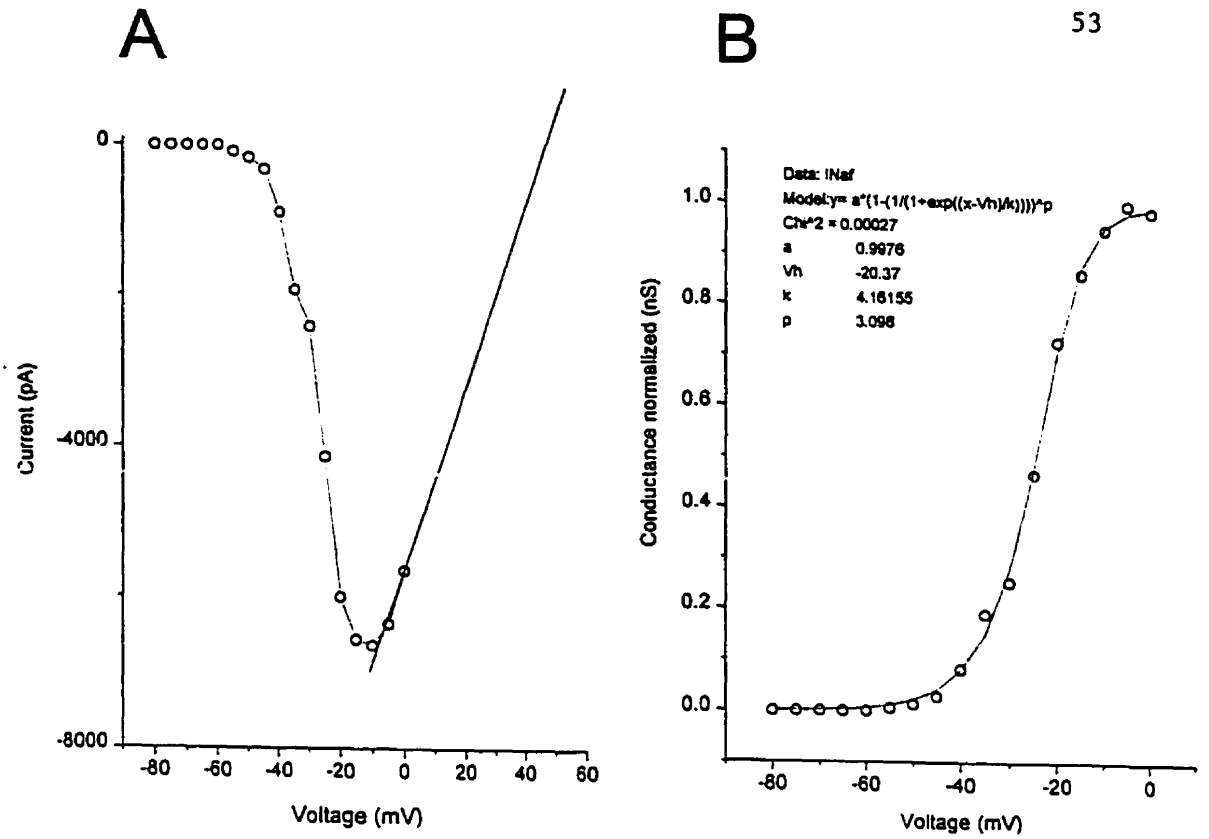

FIG. 10
A. Current-voltage relationship of the current displayed in FIG 9.
B. Activation curve obtained from the current-voltage relationship displayed in panel A.

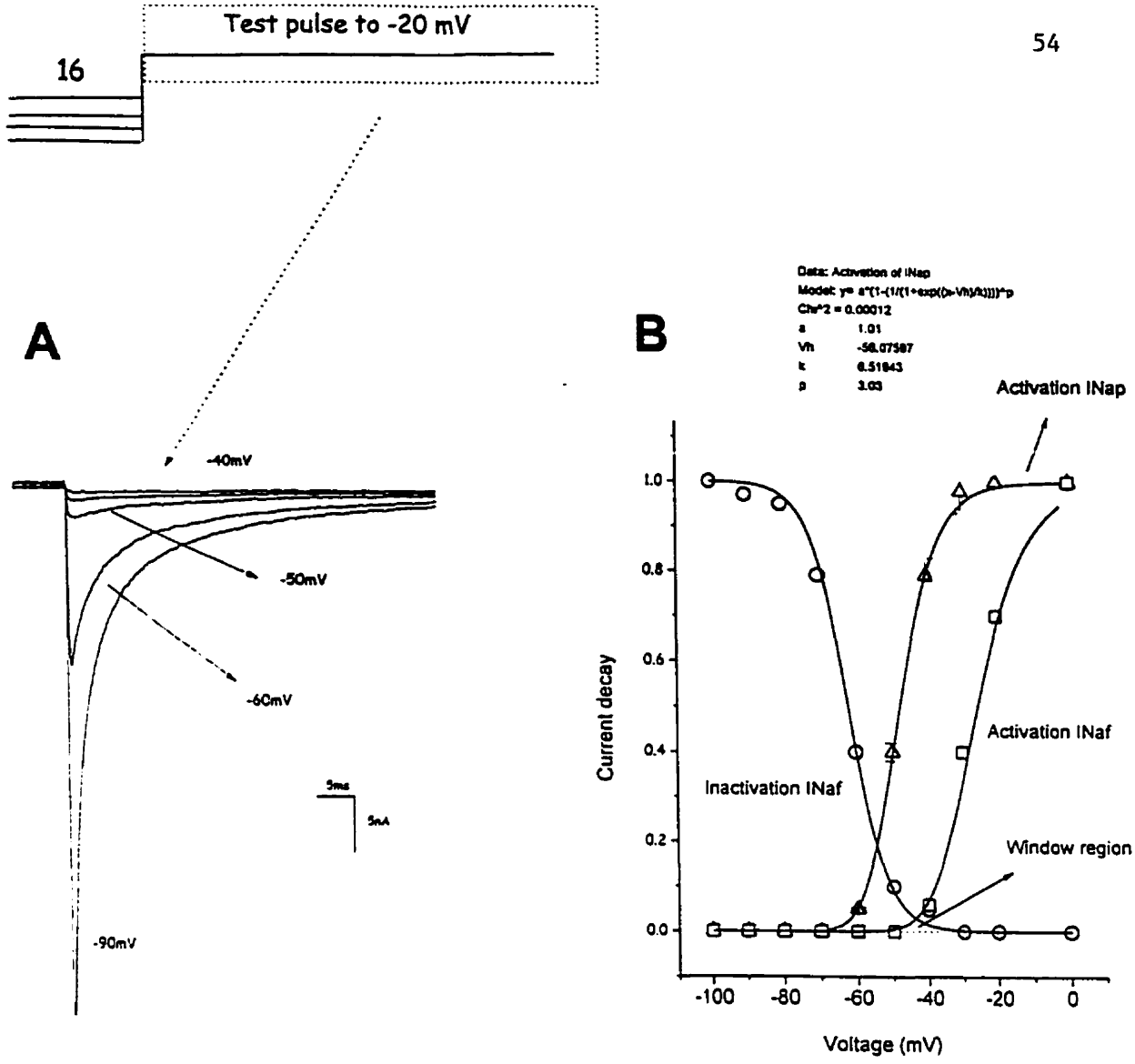

FIG 11.

A. Protocole used to study the inactivation of the transient sodium current (I_{NaF}). 100ms long prepulses were applied in 5mV steps to inactivate sodium channels. A test pulse to –20mV was then used to measure the percentage of current remaining after inactivation.
B. Inactivation curve obtained for the transient sodium current displayed in panel A. For comparison, activation curves for the transient and the persistent components are also displayed.

A

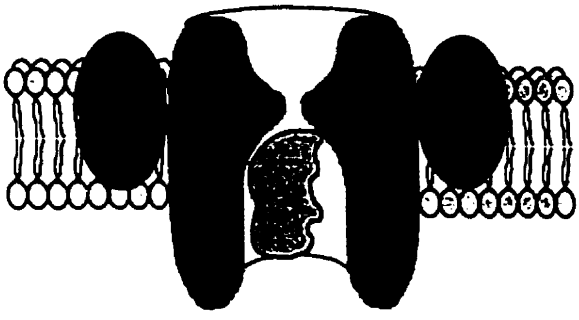

B

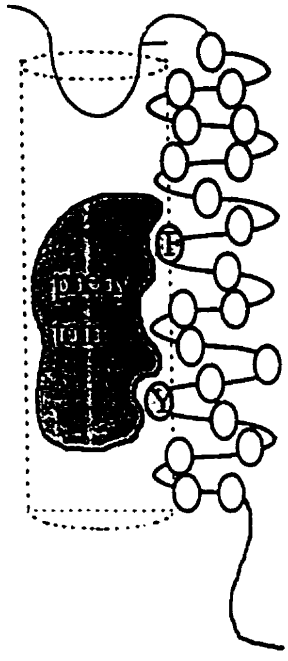

FIG. 12

A. Subunit composition of brain sodium channels. α Subunit constitutes the pore, while ß subunits modulate the channels function.
B. Expanded view of the IVS6 transmembrane segment of the α subunit. Two residues, a phenylalanine and a tyrosine are critical molecular determinants of anticonvulsant action.

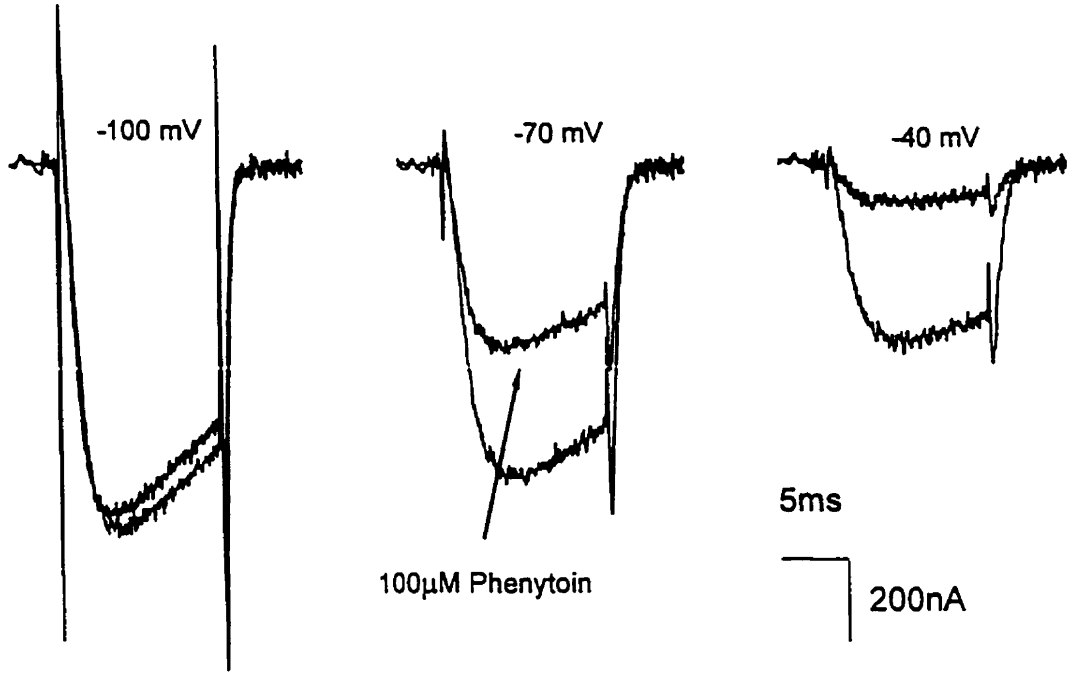

FIG. 13.

Voltage dependence of phenytoin block. Currents are evoked by a depolarizing step to 0 mv from the voltages indicated. It is evident that phenytoin block is strongly enhanced by depolarization, as illustrated when the cell is held at -40mV.

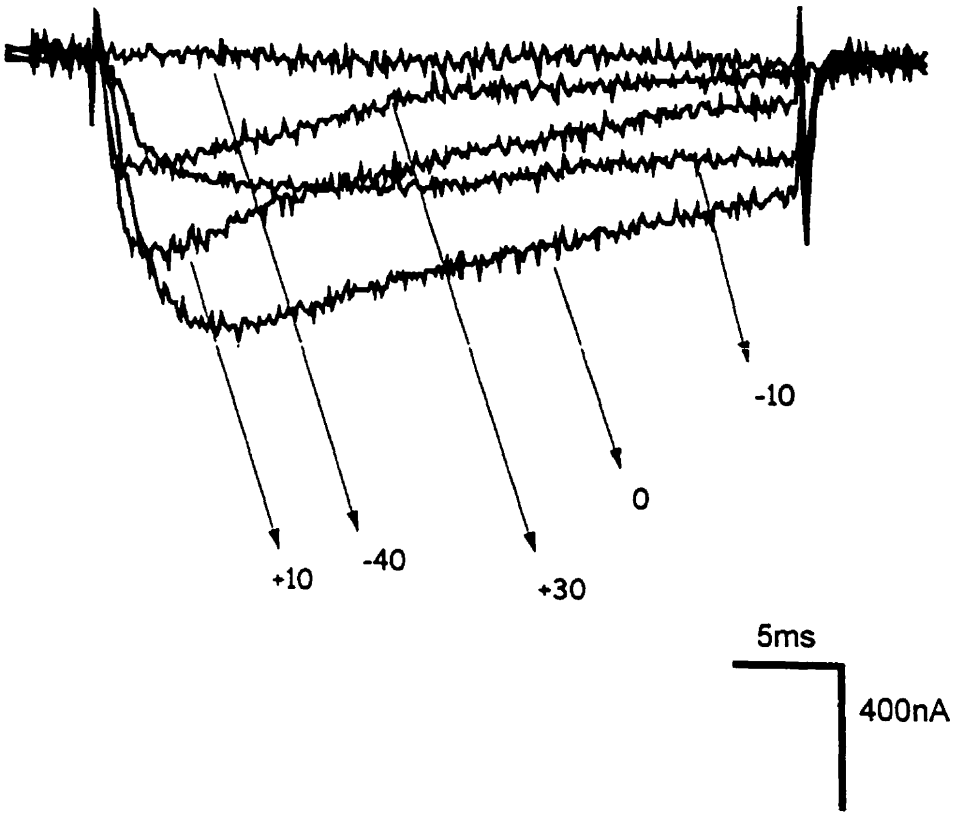

FIG. 14.

Typical record of an RIII current recorded from a *Xenopus* oocyte using the two electrode voltage clamp technique. Currents were evoked by depolarization to different potentials. Maximal currents were observed at 0mV. Holding membrane potential of the cell was -90mV.

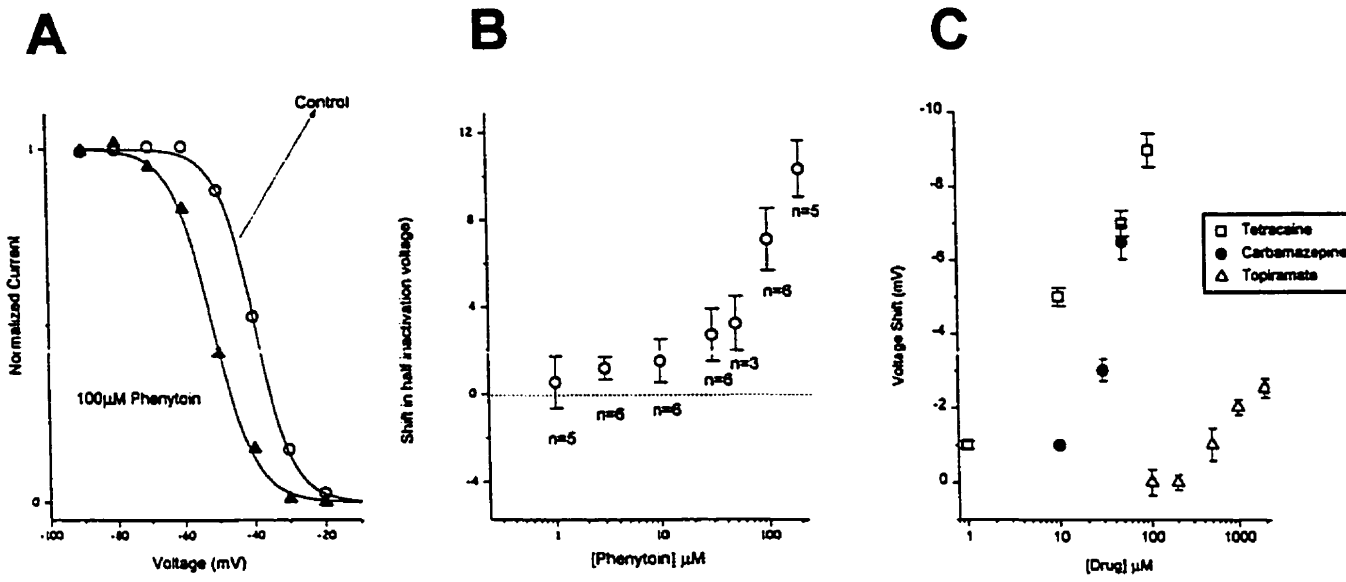

FIG. 15

A. Typical experiment illustrating the shift in half inactivation voltage (▲V ½) produced by 100µM Phenytoin. The Y axis represent availability of the channels to conduct current.
B. Cumulative results showing ▲V ½ as a function of phenytoin concentration. n represents the number of experiments performed.
C. Shifts in ▲V ½ produced by carbamazepine, topiramate and tetracaine. n is 5 for each data point.

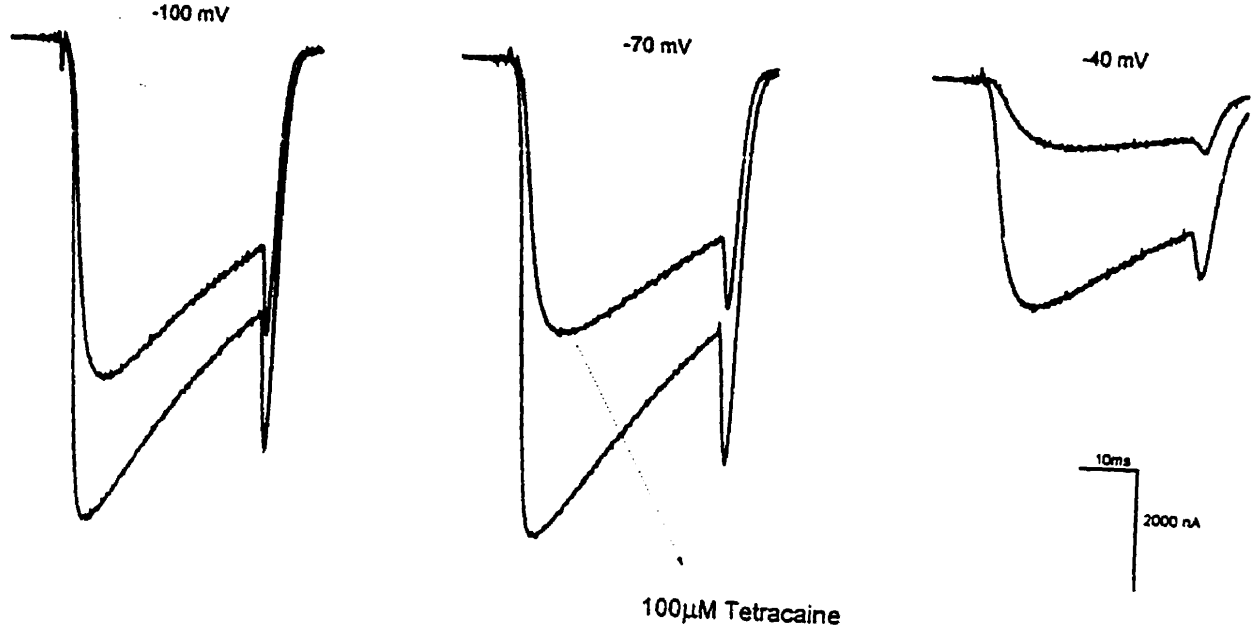

FIG. 16.

Voltage-dependence of tetracaine block of Type III sodium currents.

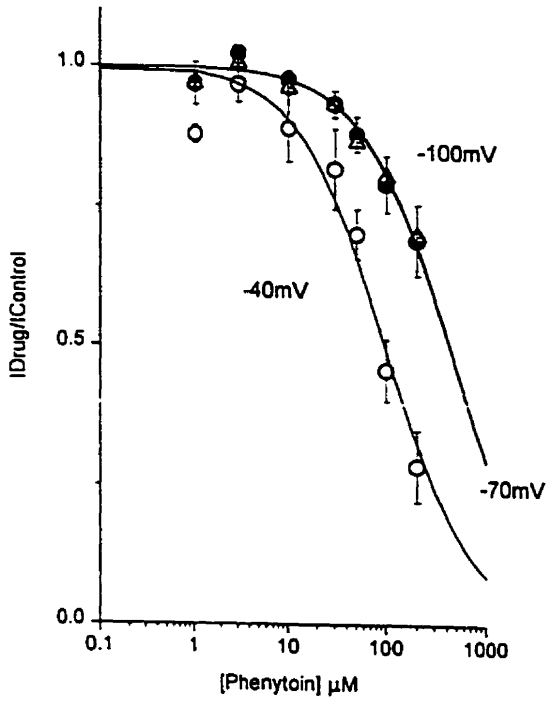

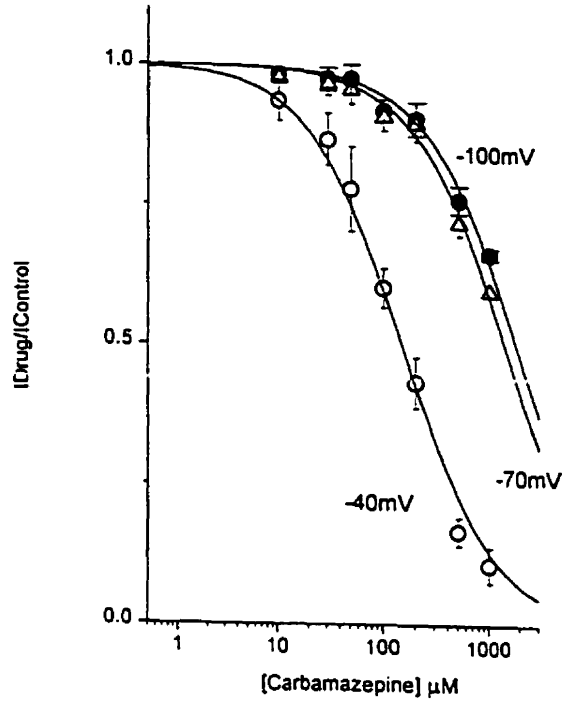

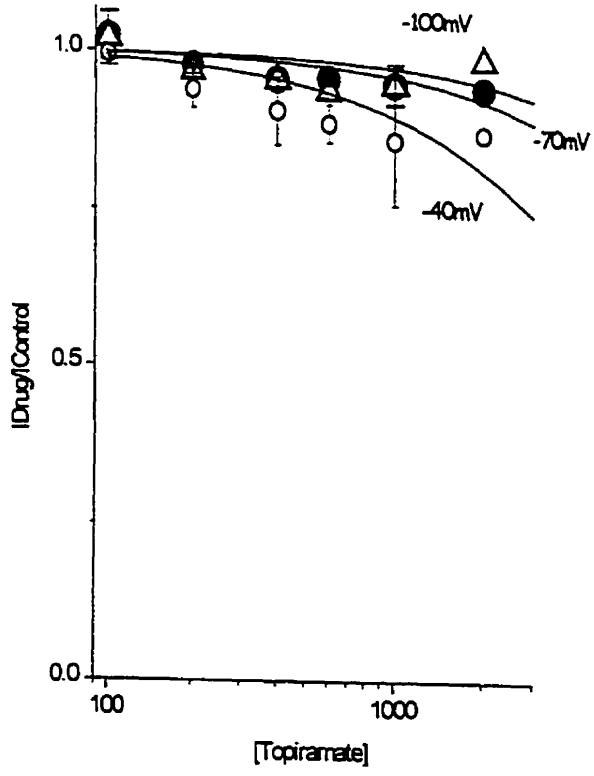

FIG. 17.

Dose response curves for inhibition of the RIII Na^+ currents by phenytoin, carbamazepine and topiramate at holding potentials of -100, -70 and -40mV. The data are the average of 10 experiments for each drug.

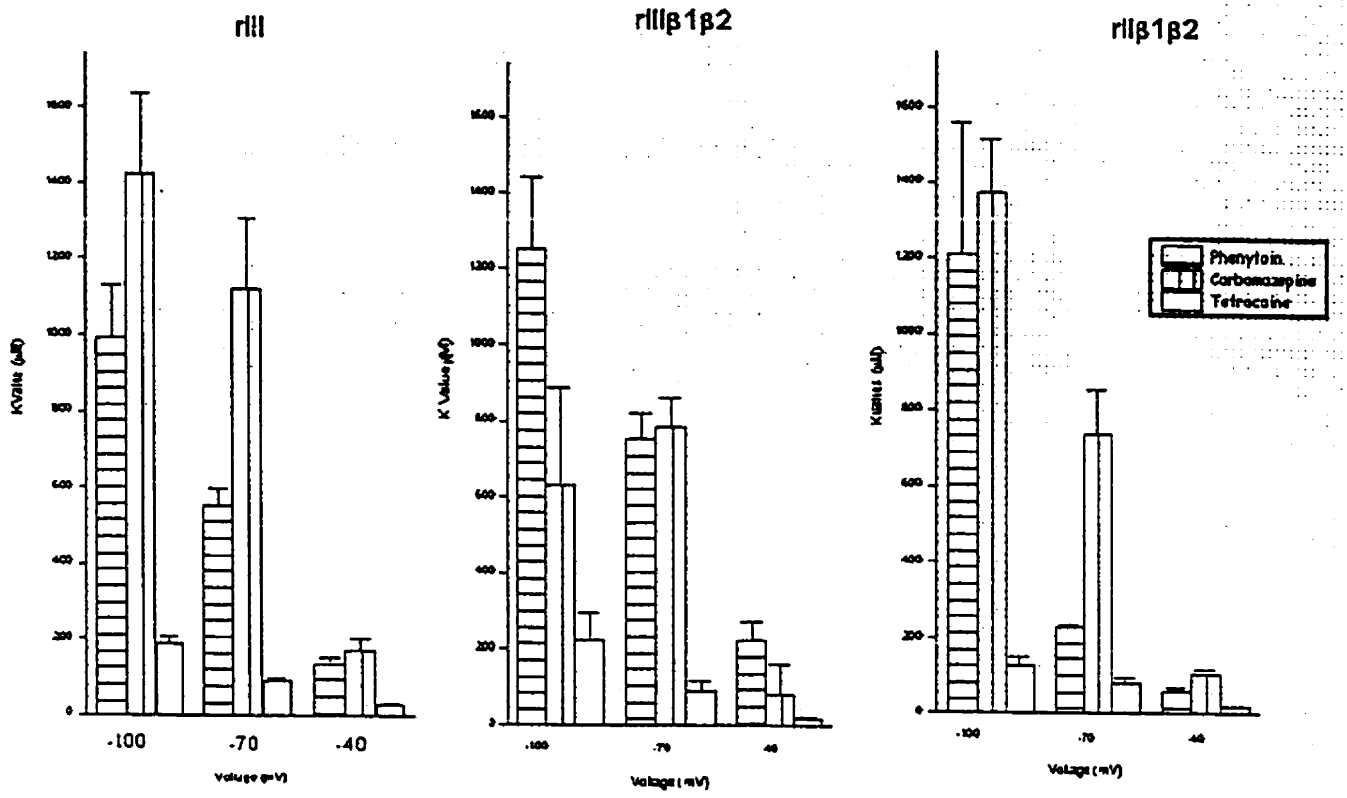

FIG. 18.

Cumulative results of dose effect experiments for rIII, rIIIβ1β2, and rIIβ1β2. The bars represent the value of the concentration (μM) that gives 50% of current block (K value).

Table 1. Cumulative values for activation and inactivation experiments carried out on the stellate cell population in the medial entorhinal cortex layer II.

Parameters ***Activation***	I_{Nap}	I_{NaF}
Number of cells analyzed	15	8
Treshold for activation (mV)	-62 +/- 2*	-49 +/- 3
Voltage value at which maximal current occurs (mV)	-35 +/- 3	-18 +/- 2
Reversal potential (mV)	33 +/- 4	39 +/- 4
Maximal conductance g_{max} (nS)	2.8 +/- 0.4	26 +/- 2
Voltage for half activation V_h (mV)	-41 +/- 5	-22 +/- 2
Slope factor (k)	6.7 +/- 1.2	5.1 +/- 1.2
Inactivation of I_{Naf}		
Number of cells analyzed		7
Voltage value required for complete inactivation (mV)		-40 +/- 2
Voltage for half inactivation V_h (mV)		-52 +/- 3

* Values are the average +/- Standard error.

Table 2. Effects of a given drug concentration on separate cells : Voltage shift for half inactivation values.

Concentration (μM)					
Phenytoin	Number of	ΔV½ (mV)	S.E	Slope Factor	
	Experiments			Control +/- SE	Drug +/- SE
1	5	0.9	1.02	5.5/0.5	4.98/0.12
3	6	1.2	0.32	5.35/0.23	5.43/0.22
10	6	1.8	0.72	5.71/0.24	5.62/0.17
30	6	2.3	0.98	5.38/0.25	5.95/0.31
50	3	3.1	0.99	5.80/0.10	6.2/0.76
100	8	6.2	1.2	5.53/0.21	6.3/0.51
200	5	10.8	1	5.71/0.08	6.71/0.33
Carbamazepine					
10	2	1.33	1.13	6.01/1.1	7.46/1.34
30	3	2.17	0.67	6.17/0.8	7.08/0.96
100	4	9.25	0.34	7.21/0.88	7.90/0.32
Topiramate					
100	4	0.1	1.3	5.04/0.14	5.4/0.32
200	3	1.1	1.2	5.01/0.24	5.1/0.32
400	2	1.59	1.1	6.45/1.1	6.23/1.3
Tetracaine					
1	3	1.03	0.22	5.74/0.35	8.13/0.48
10	3	4.94	0.65	6.41/0.41	7.27/0.76
30	3	7.23	0.54	6.5/0.29	8.25/0.16
100	3	9.08	0.17	6.17/0.32	10.38/0.43

Table 3. Complete dose-response experiments on the same cell. Cumulative values for the dose-response curves and apparent dissociation constant when RIII is expressed alone.

Phenytoin

Concentration (uM)	1	3	10	30	50	100	200
Voltage : -100mV							
ID/IC (+/- SE)	1/0.014	0.977/0.015	0.969/0.015	0.934/0.023	0.880/0.031	0.791/0.05	0.691/0.063
K Value (+/- SE)	991/139						
Voltage : -70mV							
ID/IC (+/- SE)	1/0.01	0.969/0.01	0.963/0.017	0.933/0.024	0.866/0.03	0.805/0.038	0.697/0.03
K Value (+/- SE)	553/44						
Voltage : -40mV							
ID/IC (+/- SE)	0.96/0.01	0.879/0.05	0.890/0.09	0.812/0.04	0.700/0.04	0.454/0.07	0.285/0.06
K Value (+/- SE)	136/15						
Voltage : -35mV							
ID/IC (+/- SE)	.88/0.07	0.871/0.01	0.786/0.04	0.633/0.06		0.471/0.06	0.252/0.04
K Value (+/- SE)	53/7						

Carbamazepine

Concentration (uM)	10	30	50	100	200	500
Voltage : -100mV						
ID/IC (+/- SE)	0.99/0.01	0.97/0.02	0.96/0.015	0.92/0.01	0.890/0.06	0.77/0.07
K Value (+/- SE)	1421/214					
Voltage : -70mV						
ID/IC (+/- SE)	0.98/0.02	0.97/0.03	0.96/0.05	0.91/0.04	0.88/0.043	0.71/0.09
K Value (+/- SE)	1122/183					
Voltage : -40mV						
ID/IC (+/- SE)	0.93/0.09	0.87/0.1	0.77/0.08	0.60/0.12	0.43/0.09	0.166/0.076
K Value (+/- SE)	169.4/31					

Tetracaine

Concentration (uM)	1	3	10	30	100	200	400
Voltage : -100mV							
ID/IC (+/- SE)	0.972/0.02	0.972/0.03	0.934/0.03	0.830/0.031	0.609/0.03	0.453/0.037	0.343/0.06
K Value (+/- SE)	188.6/16						
Voltage : -70mV							
ID/IC (+/- SE)	0.969/0.02	0.974/0.02	0.928/0.01	0.781/0.01	0.487/0.03	0.313/0.03	0.25/0.04
K Value (+/- SE)	90.5/6						
Voltage : -40mV							
ID/IC (+/- SE)	0.952/0.03	0.937/0.03	0.803/0.03	0.550/0.02	0.237/0.04	0.135/0.02	0.119/0.032
K Value (+/- SE)	27.9/2.8						

Table 4. Complete dose-response experiments on the same cell. Cumulative values for the dose-response curves and apparent dissociation constant for RIIIß and RIIß.

Phenytoin			
		K Value uM (+/- S.E)	
Voltage (mV)	*-100*	*-70*	*-40*
RIII B (n= 6)	1253 (186)	753.8 (68)	223.8 (51.4)
RII B (n=7)	1210 (349)	231 (4)	60 (9)
Carbamazepine			
RIII B (n=5)	635 (255)	786 (74)	81 (16)
RII B (n=4)	1369 (145)	740 (113)	108 (12)
Tetracaine			
RIII B (n= 8)	227 (67)	89 (26)	18 (3)
RII B (n=8)	127 (25)	82 (15)	19 (2)
Topiramate			
RIII B (n= 3)	4098 (578)	2980 (943)	1131 (987)
RIII (n= 2)	7098 (2456)	6976 (1345)	4879 (2457)